Energy Storage and Conversion 2025, 3(1), 1920.
https://doi.org/10.59400/esc1920

Review

A review on MXene ($Ti_3C_2T_x$) composites with varied sizes of carbon for supercapacitor applications

Ruby Garg

Independent Researcher, Cornelius, OR 97113, USA; garg.ruby251@gmail.com

CITATION

Garg R. A review on MXene ($Ti_3C_2T_x$) composites with varied sizes of carbon for supercapacitor applications. Energy Storage and Conversion. 2025; 3(1): 1920. https://doi.org/10.59400/esc1920

ARTICLE INFO

Received: 23 October 2024
Accepted: 20 October 2024
Available online: 14 January 2025

Abstract: MXenes belongs to a family of two-dimensional (2D) layered transition metal carbides or nitrides which shows outstanding potential for various energy storage applications because of their high-specific surface area, phenomenal electrical conductivity, outstanding hydrophilicity, and variable terminations. Of these different types of MXenes, the most widely studied member is $Ti_3C_2T_x$ especially in supercapacitors (SCs). However, due to the problem of stacking and oxidation in MXene sheets, significant loss of electrochemically active sites happens. To overcome these issues, incorporation of carbon materials is carried out into MXenes for enhancing its electrochemical performance. This review aims to introduce various common strategies employed in synthesizing $Ti_3C_2T_x$, followed by a brief overview of latest developments in fabricating $Ti_3C_2T_x$/carbon electrode materials for SCs. The composition of $Ti_3C_2T_x$/carbon are summarized based on different dimensions of carbons, such as 0D carbon dots, 1D carbon nanotubes and fibers, 2D graphene, and 3D carbon materials (activated carbon, polymer-derived carbon, etc.). Further, this review also aims in highlighting several insights on fabrication of novel MXenes/carbon composites as electrodes for application in SCs.

Keywords: capacitive energy storage; MXene/carbon composites; supercapacitors; synthesis process

1. Introduction

Energy is required for accomplishing every day's task. Presently, fossil fuels including oil, coal, natural gas accounts up to 80% of the total energy which adds to severe environmental pollution [1–3]. Thus, for maintaining a balance between sustainability of environment and growth of economy, wide number of articles are being published for the development of sustainable and clean energy conversion storage systems, e.g., metal-ion batteries fuel cells, capacitors and supercapacitors (SCs) [4–10]. It is highly noticeable to mention that because SCs possess superior power density (10 kW/kg) and longer cycle stability (> 10^5 cycle times) as compared to batteries, it thus helps them contributing in the areas where rapid charge–discharge, high-specific power is needed [11,12]. So, the diverse applications of these energy storage devices among various fields, such as electric vehicles, electronics, smart grid technologies and aviation have attracted their attention in the past few decades [13,14].

The classification of SCs is carried in two different categories based on their mechanism of charge storage. Out of which one is known as electric double-layer capacitors (EDLCs), in which the charge is stored physically at the interface of electrode–electrolyte via the phenomena of electrostatic attraction, which thus accounts for its superior power density [15]. For EDLCs, the most widely used electrode material is carbon-based as it possesses outstanding specific surface area for adsorbing the electrolyte ions, excellent electron conductivity, and outstanding

stability [16–18]. However, they deliver comparatively poor energy density and lesser volumetric capacitance than batteries due to low mass density of carbon [19]. The second category is known as pseudocapacitor, which involves storing charges through fast redox reactions at electrode-electrolyte interface, presenting higher energy density with lower cyclic stability and poor rate capability [20]. The most widely used materials for pseudocapacitors are transitional metal oxides/carbides, conducting polymers etc. [15,17,21–23]. It has been seen that different pseudocapacitive behaviors are resulted from the occurrence of varied faradaic processes which are classified as: underpotential deposition pseudocapacitance, redox pseudocapacitance, and intercalation pseudocapacitance [24,25]. Among these, reversible intercalation and deintercalation happens within the layered structured electrode materials in the intercalated pseudocapacitance [26,27]. To obtain the benefits of EDLCs with pseudocapacitors, researchers are on the pathway of developing hybrid SCs by integrating different combinations of materials in both the electrodes [28,29].

In SCs, the overall performance of the device is dictated by the type of electrode material used [30]. Till now, the challenges which are successfully addressed by the researchers in supercapacitor technology via different electrode materials are (i) enhancing their energy density while keeping the superior-power capability, (ii) reduction in cost with minimization in process complexity involved in manufacturing of electrodes materials, and (iii) improving their cyclic stability and life span [15,31]. In 2011, MXene is discovered in 2011 with a layered structure of two-dimensional (2D) transition metal carbides/nitrides ($M_{n+1}X_nT_x$), exhibiting greater specific surface area, higher power density, excellent electric conductivity, hydrophilicity, and functionalized surfaces [32–35]. Due to their accessibility to ions at 2D-layered structure and functionalized surface, MXenes can deliver capacitance through EDLC and pseudocapacitive phenomena, whereas in the latter method, pseudocapacitance contributes through intercalation as well as redox reactions [36–38].

The expansion of interlayer spacing in MXenes can be further enhanced by interacting with various ions, small molecules, and polymers [39–41]. This expansion in MXenes results in increased ion transport channels and decreased ion diffusion resistance, which leads in improving the overall electrochemical performance [41–44]. Moreover, MXenes also possess flexible mechanical properties, that helps them to show applications in forming binder-free and flexible electrodes [45]. Thus, MXenes has a great potential to serve as an electrode material in SCs, leading to increase in the number of publications for research articles on MXene-based SCs since 2013 [46,47]. Among various family members of MXenes, the most widely used one is $Ti_3C_2T_x$, which involves the etching of Al from Ti_3AlC_2 [41,48,49].

However, for practical applications, there are some challenges which are faced by MXenes as they are more viable for restacking and self-oxidation [34]. For instance, in $Ti_3C_2T_x$ MXene which has a layered structure obtained from etching of MAX precursor, it is important to maintain a specific layer spacing for ensuring that it should have larger specific surface area and greater electrochemically active sites. However, because of van der Waals forces, restacking happens between the individual MXene sheets, which leads to a poor accessibility of surface area and degradation in its capacitive performance [34,50]. Moreover, when there is a reaction between MXene and surrounding air or moisture, self- oxidation occurs which leads to

degradation in the performance of MXene with time. When water and air come in contact with $Ti_3C_2T_x$, nonconductive TiO_2forms due to the interaction of surface Ti atoms with oxygen or H_2O, thus reducing the electrical conductivity and capacitive active sites, leading to worsening of electrochemical performance [35–37]. Further, in SCs, when MXenes are used as an electrode material, they came across a number of challenges including severe self-discharge and a limited potential window etc. From literature, it has been anticipated that these issues still need to be addressed and investigated [39,51,52].

To mitigate the concern of restacking in MXenes, researchers are actively trying to break the restacked sheets through ultrasonication, which involves the introduction of repulsive forces between layered sheets by modifying its surface, or growing nanosheets of MXene vertically by aligning them with the substrate [26–32]. Nevertheless, even by maintaining the electron transport channels, there will be a decrease in its capacity per unit area [35–37,53]. So, the introduction of conductive spacers such as porous carbon, metal oxides/hydroxides/sulfides, conductive polymers can act as a powerful strategy in MXene nanosheets layers. This will not only prevent restacking but also helps to lead continuous electron transport channels with additional capacitance. Because of higher electron conductivity, greater surface area, excellent flexibility of carbon based materials, they are the most widely used as an electrode material. Thus, combining varied dimensions of carbon materials with MXene sheets can help in mitigating the issue of restacking. Apart from this, another benefit which carbon brings is to provide shielding against oxidation to some extent to MXenes. It's been seen from one of the research projects that on one side, it has been seen that carbon shows higher resistance to oxidation and thus helps in curbing the oxidation rates in MXenes. Whereas, on the other side, a protective layer can be formed by carbon on MXene surface for preventing oxidants e.g., contact of oxygen and water with MXene, thus reducing the occurrence of these oxidation reactions. Till date, several carbon materials are combined with varied carbon dimensions, such as zero dimensional spheres, one dimensional nanofibers or nanotubes, two-dimensional graphene nanosheets, and three-dimensional porous carbon materials are incorporated as spacers in MXene electrodes for achieving a phenomenal capacitive performance [54–56].

The following section of this review aims firstly to describe what MXenes are and then to illustrate its production methods. Further, this paper targets on giving a thorough summarization on designing and synthesizing hybrid MXene/carbon materials, along with their applications in SCs as depicted through **Figure 1**. Keeping the most widely researched $Ti_3C_2T_x$ MXene and carbon materials in mid, the classification of $Ti_3C_2T_x$/carbon is according to the dimension of carbon used is shown in **Figure 2**. The reason of incorporating carbon materials, including graphene, carbon nanotubes, or carbon dots is that they help in improving the electrical conductivity of synthesized MXene composites. These carbon materials have property of acting as a conductive scaffold thus allowing more efficient transportation of electrons, that tremendously improves the rate capability and cycling stability of the composite material. The higher surface area and hydrophilic nature of MXenes are complemented by the high conductivity of carbon materials. This hybrid thus enhances the overall capacity and stability of the synthesized material. As Carbon nanotubes (CNTs),

possesses excellent mechanical strength, it helps in stabilizing the layers of MXene and preventing the issue of restacking, thus enhancing its long-term stability.

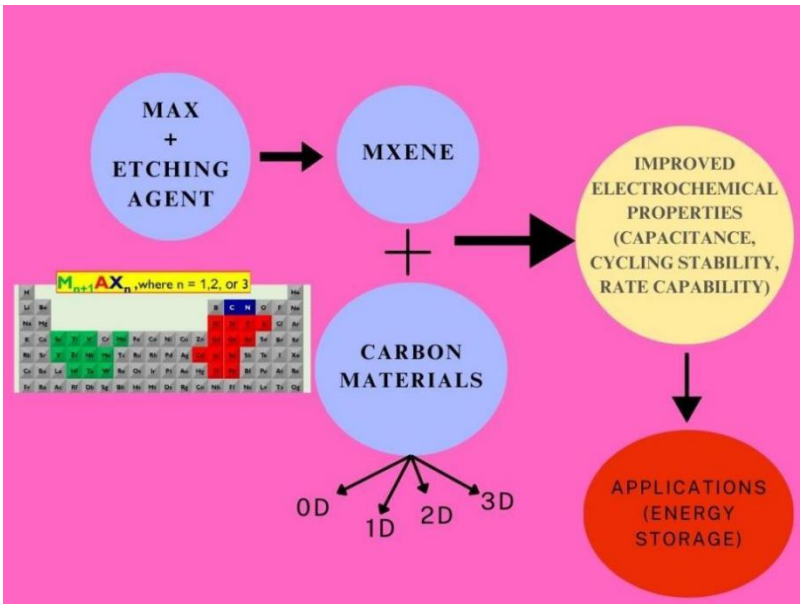

Figure 1. Improvement in the electrochemical performance of MXene/Carbon composites.

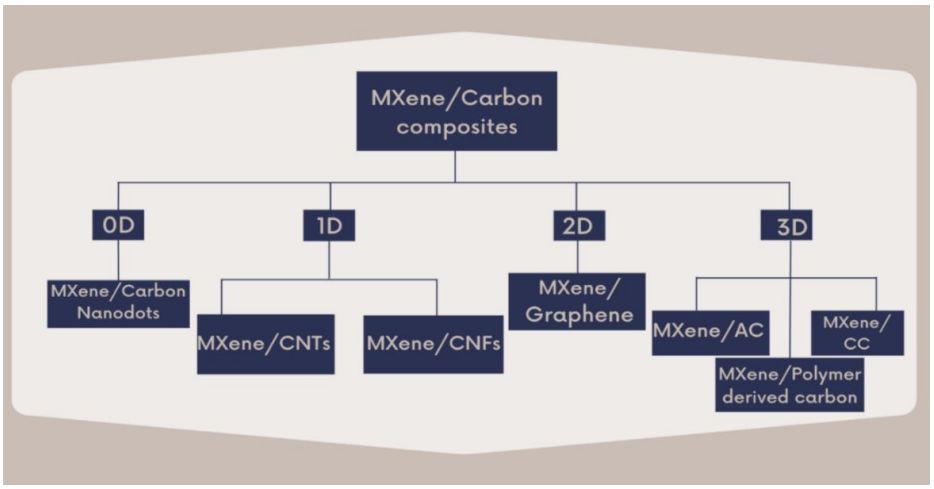

Figure 2. MXene hybrids with varied sizes of carbon as an electrode material.

With carbon materials, MXene composites gather more electrochemical active sites which means the number of charge storage sites available for ions transportation has increased. This output is highly beneficial for energy storage devices such as supercapacitors and batteries, where greater ion diffusion and higher surface area are vital for improving the overall performance. Moreover, carbon materials cycle stability also helps in mitigating the issues related to MXene degradation while cycling, such as the oxidation of the surface. The stability of carbon enhances the mechanical integrity of the composite, helping to maintain its structural integrity and prevent the loss of active material during repeated charge/discharge cycles. Ultimately, the developmental trajectory and challenges in the path of MXenes/carbon composites as electrode materials are presented to show their valuable insights and

guidance for future research endeavors. The novelty of the presented work is that the combinations of MXene with different forms of carbon (0D, 1D, 2D, 3D) for energy storage devices is achieved by tailoring the dimensionality and structure of the carbon, for creating a diverse set of composites, each optimized for specific electrochemical performance characteristics.

2. Literature survey

MXenes ($M_{n+1}X_nT_x$), belongs to a structural family of two-dimensional layered carbides and nitrides, which are selectively etched by removing elements of A-layer from ternary MAX ($M_{n+1}AX_n$) precursor using HF-containing solutions. In MAX, M signifies transitional metals including Ti, Mo, Nb, V, Cr, Zr, Ta, etc., A denotes the Group IIIA or IVA elements from the periodic table, X can have the possibility of belonging to carbon and/or nitrogen domains, and n can have the value from 1 to 4 [53,57]. In **Figure 3** periodic table has been illustrated showing the elements which are experimentally used towards the preparation of MXenes [37]. It has been seen that the adjustment in the properties of MXene either physically or chemically cannot be done by the M and X elements only but also depends on its number of layers. When value of n varies from 1 to 4 in the MAX precursor, the corresponding resulted MXenes have 3, 5, 7, or 9 atomic layers. These layers thus points to M_2XT_x, $M_3X_2T_x$, $M_4X_3T_x$, and $M_5X_4T_x$, respectively, where surface terminations are denoted by T_x which originates when A elements are removed while etching [35,36,43].

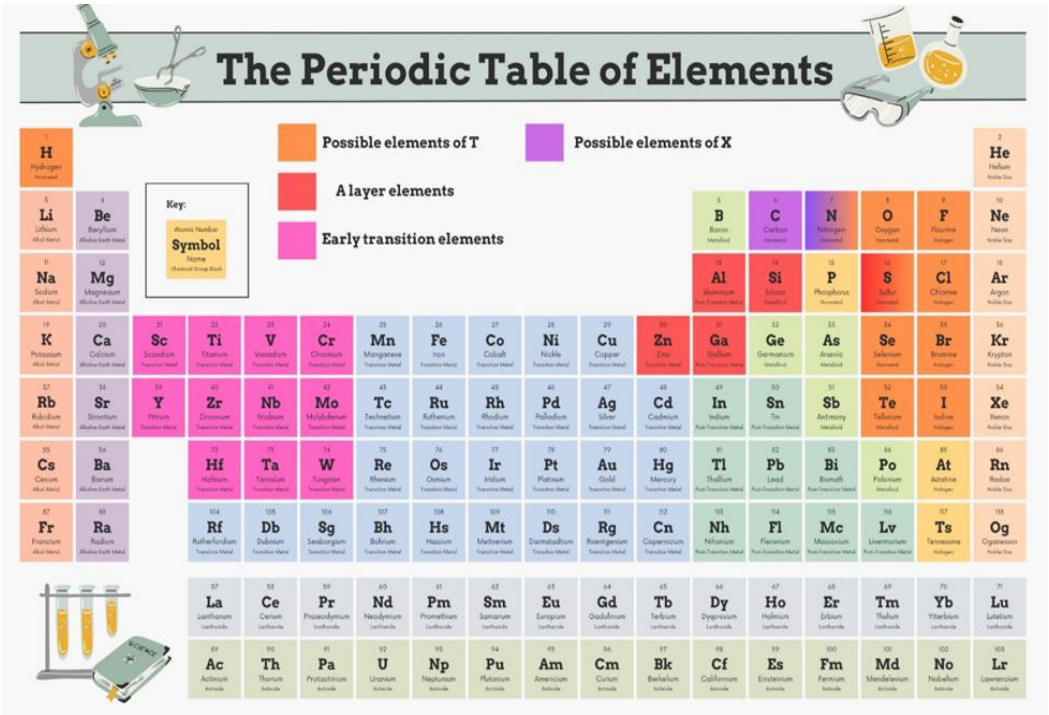

Figure 3. Contribution of the highlighted elements towards MXene preparation.

Because of 2D structures and functionalized surfaces accessibility to ions for abundant redox centers, there is a guarantee of higher energy densities and excellent rate performances in these materials. MXenes since belongs to 2D family also meet the needs of being a potential candidate to serve as an electrode material for both

EDLCs and pseudocapacitors [36]. The pseudo capacitors store charges by the process of ion intercalation and deintercalation between MXene layers. The redox reactions contribute towards the reason of pseudocapacitance. Till now there are more than 30 varieties of MXenes which have been successfully synthesized, out of which only titanium carbide is widely studied MXene by removing Al selectively from its Ti_3AlC_2 precursor for energy storage applications [49]. This is because $Ti_3C_2T_x$ possesses high-rate capability, greater specific capacitance, excellent metallic conductivity (up to 10,000 S/cm), and premium cycle stability [58]. For instance, $Ti_3C_2T_x$ MXene presents a volumetric capacitance of greater than 300 F/cm^3, which is higher than carbide derived carbons, activated graphene, graphene gel films in aqueous, and organic electrolytes [59–62]. However, it has seen realized that the different synthesis routes for $Ti_3C_2T_x$ directly affects the generation of surface functional groups, sheet size, spacing between its layers, and energy storage value [61]. So, it is vital to find effect of these synthesis methods on physical, chemical, and electrochemical performances of fabricated $Ti_3C_2T_x$.

2.1. Different methods to fabricate MXene (Ti_3C_2Tx)

The categorization in the synthesis methods of $Ti_3C_2T_x$ are carried into "bottom-up" and "top-down" methods as shown in **Figure 4**.

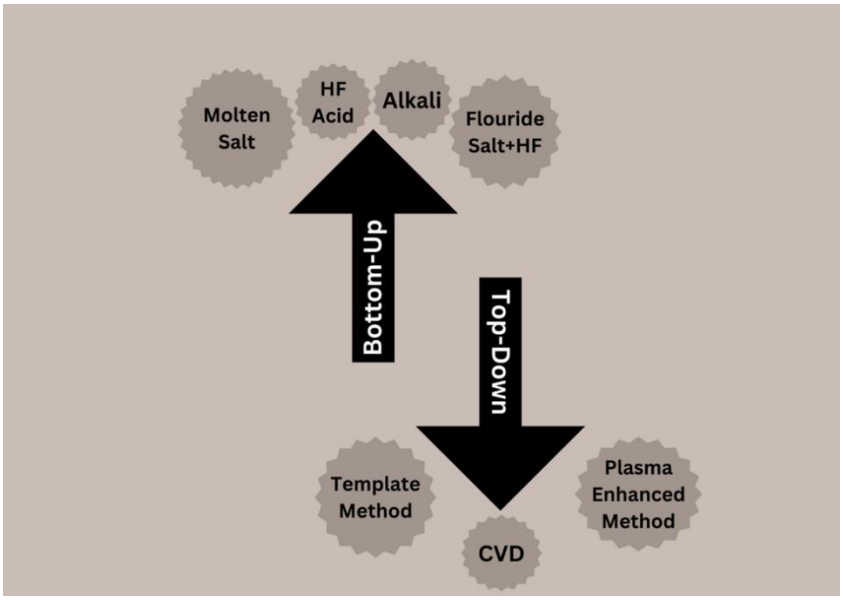

Figure 4. Illustration of bottom-up and top-down approaches for successful synthesis of MXene.

The bottom-up approach involves synthesizing MXene thin films from small components whereas in top-down approach, MAX precursor exfoliation is carried out. The bottom-up strategy is more controlled which involves the generation of MXene epitaxial films with few layers. For instance, MXene thin films are produced through the method of chemical vapor deposition (CVD). In this process, substrate and MXene precursor are heated at a specific temperature, resulting in the decomposition of precursor to desired MXene species. These species are then deposited on substrate surface to prepare thin films. In CVD technique, high purity products are produced

with definite functional groups as it is a fluorine-free method [37]. However, the drawback in bottom-up approach is that the output is low, and the process is tedious. Further, in the top-down method the etching of 3D Ti_3AlC_2 accounts in forming accordion like structure or flaky 2D $Ti_3C_2T_x$ films, whereas bottom-up strategy yields to few-layer $Ti_3C_2T_x$ thin films directly using CVD [52]. The step-by-step guide to the synthesis of MXene through both these processes is depicted in **Figure 5a,b**. In this section, most of the discussion is carried in detail about the etching agents for the preparation of $Ti_3C_2T_x$ as most of the synthesis is done through "top-down" methods.

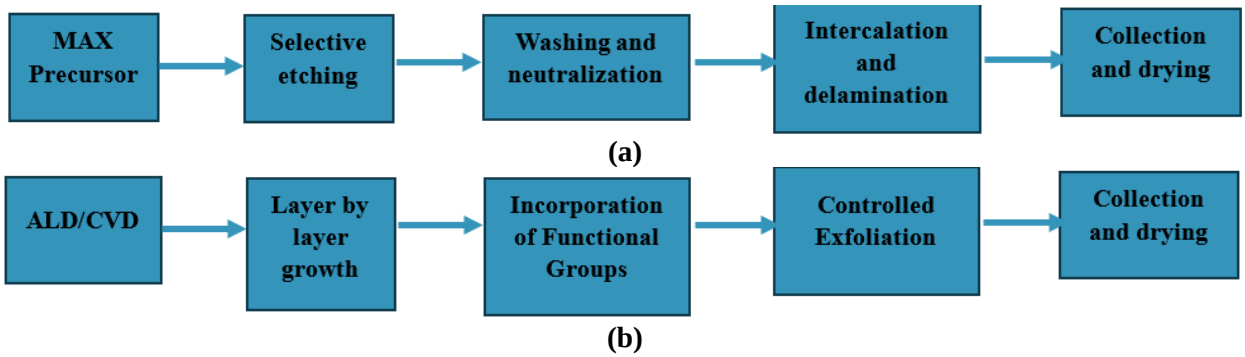

Figure 5. (a) Step and step illustration of top to bottom approaches for successful preparation of MXene; **(b)** step and step illustration of bottom to top approaches for successful preparation of MXene.

2.2. Etching MAX precursor using HF

The most widely studied and earliest method used for the synthesis of MXene from MAX precursor is etching with HF [63]. Research carried by Naguib et al. [47,64] showed the successful preparation of multilayer MXene from Ti_3AlC_2 MAX precursor by utilizing 50% HF for 2 h at room temperature. Equations (1)–(3) show the reactions involved in its synthesis [64]. After etching, sheet like 2D MXene powder is produced in which different layers connect to each other through van der Waals forces and hydrogen bonds. The deionized water is then used to wash off the residual acid followed by vacuum drying.

$$Ti_3AlC_2\,(s) + 3HF\,(aq) \rightarrow Ti_3C_2\,(s) + AlF_3\,(aq)\,(1) + 3/2H_2\,(g) \quad (1)$$

$$Ti_3C_2\,(s) + 2HF\,(aq) \rightarrow Ti_3C_2F_2\,(s) + H_2\,(g) \quad (2)$$

$$Ti_3C_2\,(s) + 2H_2O\,(l) \rightarrow Ti_3C_2(OH)_2\,(s) + H_2\,(g) \quad (3)$$

Similarly, MXene synthesis has been successfully shown by Naguib et al. [65] by mixing 2 g of MAX (Ti_3AlC_2 (400 mesh)) with 400 mL of HF. From his study on XRD patterns, it has been anticipated that in exfoliated 2D $Ti_3C_2T_x$ layers, Ti atoms are exposed forming hydroxylated $Ti_3C_2(OH)_2$ and fluorinated $Ti_3C_2F_2$. The accordion shape of $Ti_3C_2T_x$ is also proved from the scanning electron microscope (SEM) image [64]. Further, the effect of delamination and varied etching agents has been shown by Alhabeb et al. [66] on the synthesis of $Ti_3C_2T_x$. It has been shown in their study that for etching Al from MAX phase 5 wt% of HF solution is sufficient however, for achieving accordion like structure, minimum concentration of HF should be 10 wt%. Nevertheless, the greater usage of HF in these experimental processes strives towards greater health risks because of its corrosive nature and strong odor. Moreover, because

of this the synthesized $Ti_3C_2T_x$ possess various defects, which results in instability of its structure.

2.3. Etching MAX precursor using acid/fluoride

To mitigate the issue of using HF directly, researchers are trying to etch A layer from MAX precursor by mixing strong acid with fluoride salt. Fluoride salts involve LiF, NaF, KF, NH_4HF_2, KHF_2, $NaHF_2$, and NH_4F, and strong acids include HCl and H_2SO_4 [47,65,67,68]. Presently, the widely explored etching agent is a solution of HCl and LiF. The equation showing this reaction is as follows:

$$LiF\ (aq) + HCl\ (aq) \rightarrow HF\ (aq) + LiCl\ (aq). \quad (4)$$

In one of the studies shown by Ghidiu et al. [66], LiF is dissolved as an etching agent in a 6 M HCl solution. To this salt mixture, the addition of Ti_3AlC_2 MAX was performed gradually, and the temperature of this solution was maintained at 40 ℃. The precipitation thus formed went under filtering and washing repetitively with deionized water. In this state, the deposit that was fabricated has a clay like appearance which allows it to be rolled either to a free-standing film or into various other shapes [66]. The results of X-ray diffraction (XRD) patterns showing the effect of LiF–HCl etchants on before and after had proved to turn $Ti_3C_2T_x$ to $Ti_3C_2F_2$. Like the HF etching, the proportion of adding LiF into HCl also played a major role in maintaining the structure and size of $Ti_3C_2T_x$. Further, one more benefit of using LiF salt is that cations such as Li^+, Na^+, K^+, and NH_4^+ can be easily intercalated into MXene layers for expanding its layer spacing. This enhancement in the spacing of MXene layers allows the accessibility of higher redox active sites for promoting the ion transport rate and increasing its capacitive performance volumetrically. Also, with this approach, any major damage to the structure of $Ti_3C_2T_x$ should also be prevented.

2.4. Etching MAX precursor using alkali

Concerning about safety and pollution of the environment, researchers are devoting their valuable time towards finding HF-free etching agents [47,65,67] It has been discovered that a concentrated sodium hydroxide's deoxygenated solution have the tendency of etching Ti_3AlC_2 through the processes as shown in the following formulas:

$$Ti_3AlC_2\,(s) + OH^-\,(aq) + 5H_2O\ (l) \rightarrow Ti_3C_2(OH)_2\ (s) + Al(OH)_4\,(aq) + 5/2H_2\,(g) \quad (5)$$

$$Ti_3AlC_2\,(s) + OH^-\,(aq) + 5H_2O\ (l) \rightarrow Ti_3C_2O_2\ (s) + Al(OH)_4\,(aq) + 7/2H_2\,(g) \quad (6)$$

Xie et al. [69] used NaOH solution for immersing large pieces of MAX precursor for the surface treatment, followed by treating it with H_2SO_4 hydrothermally for obtaining Ti_3C_2 layers terminated with hydroxyl groups. Thus, **Table 1** briefly summarizes the etching conditions and capacitive results of fabricated $Ti_3C_2T_x$ from the usage of different etching agents.

Table 1. Illustration of MXene performance in different etching solutions as an electrode material.

Electrode material	Etchant solution	Mass loading (mg/cm^2)	Specific capacitance (F/cm^3)	Scan rate (mV/s)	Capacitance retention (%)	References
$Ti_3C_2T_x$	HCl/LiF	1.85	910	3	100	[66]
d- $Ti_3C_2T_x$	HF	1.296	520	3	100	[70]
KOH 400- $Ti_3C_2T_x$	HF	-	517	1	99	[71]
$Ti_3C_2T_x$	NaOH	8.476	511	2	89	[72]
$Ti_3C_2T_x$ hydrogel	HCl/LiF	5.3	1500	2	90	[73]
$Ti_3C_2T_x$ hydrogel	HCl/LiF	-	226	2	97	[74]
$Ti_3C_2T_x$	HF/HCl	1	1200	5	-	[75]
$Ti_3C_2T_x$	HF/HCl	12	649	5	99	[62]

2.5. Etching MAX precursor using molten salt

Recently, MAX phase etching has been registered through a new procedure following molten salt [37]. Li et al. [76] etch Ti_3AlC_2 using a mixed $ZnCl_2$/NaCl/KCl molten salt system under an atmosphere of nitrogen. For MAX phase, $ZnCl_2$ is used as an etchant together with the bath formation of molten salt comprising NaCl + KCl because of its lower melting point. In this process, Zn^{2+} ions reaction occurs with A atoms of the MAX phase which replaces these lattice sites of A-layer elements leading to fabrication of new Zn-MAX phases. The interlayer Zn atoms are subsequently removed by excess $ZnCl_2$ from Zn-MAX phase, resulting $Ti_3C_2Cl_2$ MXene. The description of above etching process is depicted below:

$$Ti_3AlC_2 + 3/2ZnCl_2 \rightarrow Ti_3ZnC_2 + 1/2Zn + AlCl_3. \text{ (7) } Ti_3AlC_2 + ZnCl_2 \rightarrow Ti_3C_2Cl_2 + 2Zn. \quad (7)$$

Since, a wider etching and more safety is offered by nonaqueous molten salt solution, it was thus synthesized at an early stage and needs further deep research on its impact on physical and chemical properties of the synthesized MXene such as electric conductivity, hydrophilicity, and mechanical properties etc.

2.6. Other alternatives for MXene synthesis

In an electrochemical etching method, MAX phase is treated with a specific voltage, that works as a working electrode. Sun et al. [77] in their study chose titanium aluminum carbide (Ti_2AlC) as a working electrode, silver/ silver chloride (Ag/AgCl) as reference and Platinum as the counter electrode under a three-electrode system along with hydrochloric acid as an electrolyte. It has been discovered from this research when etching was performed electrochemically at a working voltage of 0.6 V vs. Ag/AgCl few of the titanium elements got eliminated, along with the formation of carbide-derived carbon (CDC) both of which helped in hindering the further etching. Although the process of electrochemical etching operates at lower temperature with low energy consumption, but the formation of CDC layers on MXene restricts its etching process with lower output [77]. Hence with this method, large-scale preparation of MXenes is highly unstable.

Afterwards, Halogen has also been introduced as a new alternative to an etchant. Shi et al. [78] synthesized accordion-like $Ti_3C_2I_x$ by utilizing I_2 for etching Ti_3AlC_2 at

100 ℃ in an anhydrous acetonitrile (CH_3CN). Additionally, it also has been considered that the mechanical, electrical and magnetic waves are used for etching of layered ternary precursors. In one of the research projects carried by Yang et al. [79], the usage of fluorine-free etching method is demonstrated in which anodic corrosion of Ti_3AlC_2 is conducted in an aqueous binary electrolyte solution of 1 M NH_4Cl and 0.2 M tetra- methylammonium hydroxide having pH > 9. This technique showed chances of mono or bilayer MXene ($Ti_3C_2T_x$) nanosheets production under five hours of secured etching environment. Further, it has been illustrated from Zhang et al. [80] study that a large-scale synthesis of few-layer $Ti_3C_2T_x$ powders were carried by employing liquid-based flocculation methods. This method has considerably limited the preparation time along with improving the output of resulting few-layered MXene powders. Thus, the method of liquid-phase flocculation holds a great importance in MXene synthesis.

3. Methods of fabricating MXene composites with varied sizes of carbon as an electrode material for supercapacitor applications

Excellent mechanical, thermal and chemical stabilities, higher porosity, and great conductivity shown by carbon-based materials make them a versatile candidate to be used as an electrode material [57]. As Carbon have tons of functional groups present on their surface, it allows them to form various covalent bonds or van der Waals force bonds with different guest substrates [81–84]. Thus, it is extremely useful if MXene/carbon composites are fabricated as electrodes in supercapacitors [24,54]. Thus, in the below sections, composites of $Ti_3C_2T_x$/carbon are carefully introduced according to the varied dimensions of the carbon materials. The performance shown by $Ti_3C_2T_x$/carbon electrodes in recent years for SC applications is illustrated in the following sections. Few more research articles are included for comparison in the **Table 2** illustrating the improvement in the performance of MXene by synthesizing its composites with varied sizes of carbon.

Table 2. Electrochemical performance comparison of MXene with different dimensions of carbon.

Material	Carbon Size	Specific Capacitance (F/g)	Rate Capability (1 A/g)	Cycling Stability (after 1000 cycles)	Energy Density (Wh/kg)	Power Density (W/kg)	References
Bare MXene (Ti_3C_2)	-	256	68%	85% after 1000 cycles	25	650	[81]
MXene-Carbon Nanodots (CND)	0D	330	70%	90% after 1000 cycles	30	700	[85]
MXene-Carbon Nanotubes (CNT)	1D	375	80%	95% after 1000 cycles	35	750	[86]
MXene-Graphene	2D	450	85%	98% after 1000 cycles	40	800	[87]
MXene-Activated Carbon	3D	420	75%	95% after 1000 cycles	45	850	[88]
MXene-Graphene Composites	2D	430	83%	97% after 1000 cycles	38	780	[89]

3.1. 0D carbon/$Ti_3C_2T_X$ composites

Carbon dots (CDs) stand for 0D carbon material which has gathered spectacular attention in past few years [90]. When their composites are formed with MXene, these miniaturized CDs have the property of dispersing easily all over on the flat surface of MXene which helps in preventing the issue of restacking in MXenes and exposure of more active sites for electrolytic ions to diffuse inside these MXene sheets. Thus, it helps in enhancing the energy density of supercapacitors if the composition of these composites is employed as electrode materials. Findings prove that specific capacitance and cycle retention of MXene/CDs composites is better than if these are used as individual components [91–93]. Thus, this section discusses the synthesis techniques, structure properties, and electrochemical results of MXene/CDs composites in detail.

A simple and effective method has been developed by Li et al. [91] to fabricate hybrid CDs and $Ti_3C_2T_x$ films as SC electrodes as depicted through **Figure 6**. Wheat straw, Enteromorpha proliferate, pomelo juice, and tribute chrysanthemum, were the four precursors that used for the synthesis of CDs. Afterwards, $Ti_3C_2T_x$/CDs composite films were prepared by the incorporating CDs into $Ti_3C_2T_x$ suspension. The enhancement in the electrochemical performance has been obtained by optimizing the composite film, that was prepared by using 5 wt.% of pomelo juice-derived CDs with nitrogen/sulfur doping (NSPJCDs) along with 95 wt.% of $Ti_3C_2T_x$ as shown in **Figure 7**.

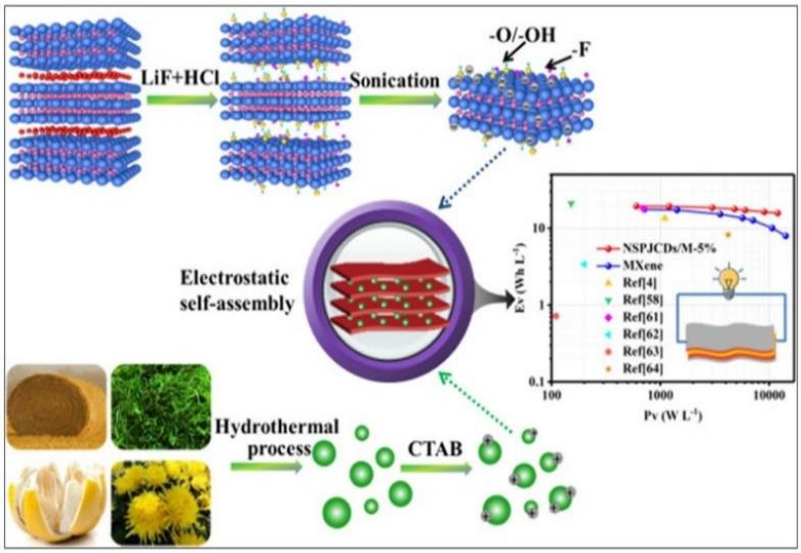

Figure 6. Synthesis process of CDs and $Ti_3C_2T_x$ films [91].

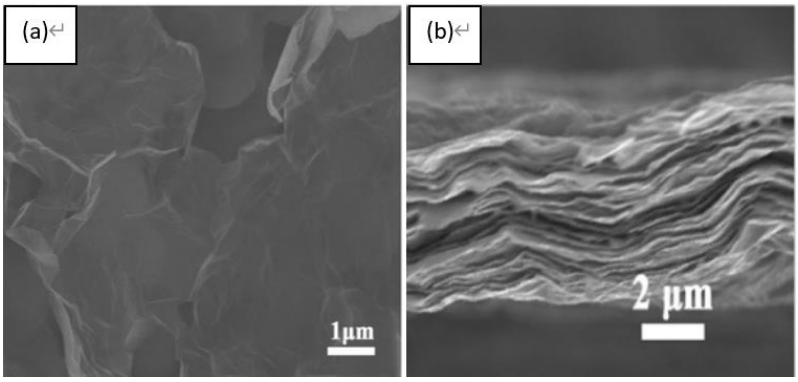

Figure 7. SEM images of **(a)** $Ti_3C_2T_x$, **(b)** NSPJCDs-M (5%) [91].

From the SEM results, it has been seen that 1.41 nm of interlayer spacing has been achieved in **Figure 7b** with the composite film which was 1.26 nm in pure MXene film as shown through **Figure 7a**. This enhanced spacing has helped in obtaining greater accessible electroactive sites which thus boost the diffusion distances and transportation of ions. Results showed that $Ti_3C_2T_x$/CDs composite electrode exhibits a gravimetric capacitance of 327.1 F/g, and the nonlinearity in the curves of galvanostatic charge–discharge (GCD) represent the pseudocapacitive behavior. Additionally, excellent cycling stability, and capacitance retention with a value of 94.6% was obtained after 10,000 cycles. Moreover, this hybrid supercapacitor also displayed an energy density of 6.45 Wh./kg with a power density of 200 W/kg. However, in this study the performance of composite has been highly dependent on the size of the carbon dots incorporated. Too much or too little carbon dot incorporation could have the adverse effects on the overall performance of the material as it is more difficult to control its parameters during practical applications as the tendency of carbon dots depends mainly on their concentration as well as distribution within the MXene matrix.

One more research by Tan et al. [94] utilized 0D carbon dots and 2D MXene nanosheets for producing $Ti_3C_2T_x$@CDs composite electrode material. A hydrothermal method is employed for the successful synthesis of CDs at a temperature of 200 ℃ for 300 min from a mixture of m-phenylenediamine and diethyl-netriaminepenta solution. Then the addition of CDs was done into $Ti_3C_2T_x$ suspension for synthesizing stable and flexible $Ti_3C_2T_x$@CDs hybrid films via a process of vacuum filtration. However, as MXenes are highly prone to issues like oxidation and surface termination loss when exposed in aqueous solution over time. Although this study presents promising results, but the long-term stability of the synthesized micro flowers remains unclear for real-world applications.

The bonding between MXene and carbon dots can be ascribed because of their electrostatic interaction as $Ti_3C_2T_x$ possesses a zeta potential of −29.3 mV, whereas CDs reflects a zeta potential of +36.8 mV. Study by Zhang et al. [95] proposed an intercalation strategy for fabricating flexible MXene based thin film electrodes by incorporating calcium alginate (CA) into MXene nanosheets, followed by carbonization. It has been seen from this research that because intercalating and evaporating CA hydrogel within $Ti_3C_2T_x$ nanosheets yielded in high density $Ti_3C_2T_x$/CA films. The increase in spacing between MXene layers was possible

through the process of carbonization due to which MXene nanosheets have CA-derived carbon dots inserted in their layers thus promoting the electrolyte ions diffusion inside of MXene film as shown through **Figure 8**. For this reason, $Ti_3C_2T_x$ films embedded by CDs displayed an outstanding capacitance of 1244.6 F/cm^3 at a current density of 1 A/g, a superior rate capacity of 662.5 F/cm at 1000 A/g, and a capacitance retention of 93.5% after 30,000 cycles in 3 M H_2SO_4.

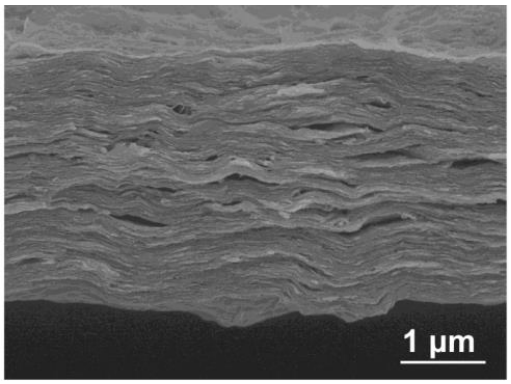

Figure 8. Cross-sectional SEM image of the MXene/CA film.

Thus, this listed study has provided a simple and cost-effective strategy for building hybrid MXene/carbon thin film electrodes with excellent storage capacity. On the other hand, the key feature in electrode materials is their flexibility, however there can be a trade-off between flexibility and performance. For instance, electrochemical performance in some situations got reduces if the material is too flexible. Thus, balancing in maintaining mechanical flexibility along with achieving high electrochemical performance is yet to be explored.

3.2. 1D carbon nanotube (CNTS) or fibers/$Ti_3C_2T_X$ composites

Irrespective of carbons alternatives, one dimensional (1D) carbon, involving carbon nanotubes (CNTs), carbon nanofibers (CNFs) and carbon tubular superstructures, might also be considered as self-standing materials without a need of binders or substrates, and hence helps in forming highly conductive networks via the interactions among wide range of carbon materials [81,95–100]. Because of the smooth pathways offered by 1D materials, researchers have investigated from the measurements and simulations that ions and electrons movement through 1D carbon materials is exceptionally fast [101]. Further, the robustness of the mixture can also be ensured due to the superior mechanical strength of 1D structures. In flexible SC systems, the unique structure of 1D carbon can also mitigate issues caused under harsh test conditions [102]. Thus, these 1D carbon materials are perfect candidate to be used as spacers for stabilizing MXene electrode's structure.

3.2.1. Investigating $Ti_3C_2T_X$/CNT composites

Carbon nanotubes referred to as (CNTs) could be recognized as twisted graphene sheets which are categorized into single walled carbon nanotubes (SWCNTs) and multiwalled carbon nanotubes (MWCNTs) depending upon the number of layers of graphene. SWCNTs surface is simple and inert in nature whereas MWCNTs are highly reactive with a greater number of defects because of the increase in the wall layers

[95]. The incorporation of 1D CNTs in $Ti_3C_2T_x$ MXene, not only enhances flexibility but also prevents restacking by acting as a conductive spacer [103]. Moreover, the electrolyte ion diffusion, electron transport, and electrochemical performance has also been promoted as CNTs behave as a viaduct between nanosheets of MXene [81].

Yang et al. [95] used an electrophoretic deposition method (EPD) for preparing $Ti_3C_2T_x$/CNT composite films on graphite substrate. It can be seen from the results that the specific gravimetric capacitance displayed by $Ti_3C_2T_x$/CNTs hybrid film was 134 F/g at a current density of 1 A/g that is nearly 1.5 and 2.6 times greater than that delivered by bare $Ti_3C_2T_x$ and CNTs film, respectively. Moreover, the $Ti_3C_2T_x$/CNTs electrode performance was highly impressive as no decay was observed in the capacitance for over 10,000 cycles, which signifies increased ions accessibility to the film of the composite ($Ti_3C_2T_x$/CNTs) material. Later, cyclic voltammetry (CV) and galvanostatic charge-discharge (GCD) of symmetrical $Ti_3C_2T_x$/CNTs supercapacitor was characterized and found to have the specific capacitance of 55.3 F/g with an energy density of 0.56 Wh/kg and power density of 416.7 W/kg at 5 A/g. Similarly, Li et al. [94] presented research where they synthesize Ti_2CT_x MXene with the help of HCl and LiF etchant. Afterwards, CNTs were mixed with synthesized MXene for obtaining Ti_2CT_x MXene/CNTs nanocomposite "paper". Through electrochemical measurements, this "paper" showed excellent capacitive results with the value of specific capacitance as 515.3 F/g and volumetric capacitance as 694 F/cm^3 at a scan rate of 2 mV/s. However, while preparing MXene/CNT films, there might be a trade-off in film thickness and electrochemical performance. The overall performance can be affected negatively if films are thicker films as they highly impact the charge transportation and ion diffusion. Thus, it's a challenge in obtaining an optimal film thickness which balances electrical conductivity, capacitive performance, and mechanical stability.

Thereafter, Li et al. [104] built a new simple alkali-induced method for preparing porous $Ti_3C_2T_x$/CNT film (known as A-MCF) as shown through **Figure 9**. In the resulting film, after the introduction of CNTs, issues of restacking in $Ti_3C_2T_x$ nanosheets were successfully addressed, thus efficiently promoting utilization of the active sites on MXene surface resulting in fast ion/electron transportation.

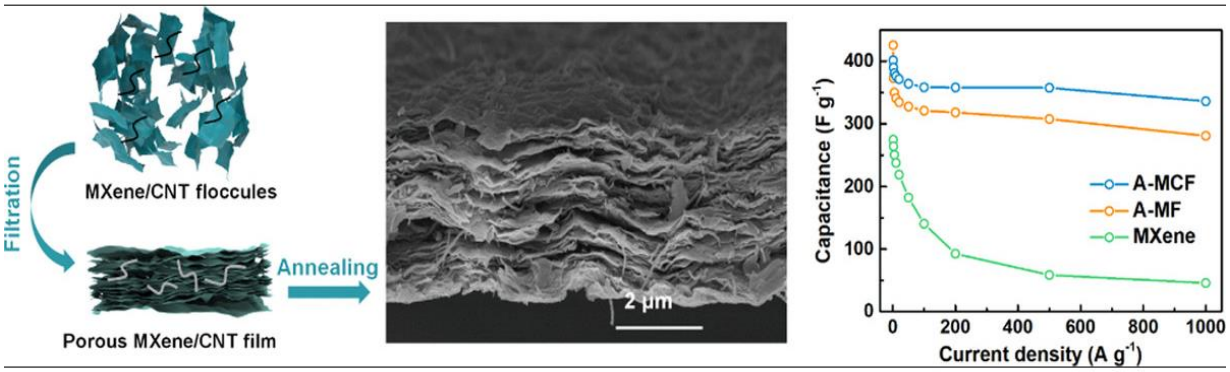

Figure 9. Effect of alkali-induced method for preparing porous $Ti_3C_2T_x$/CNT film [99].

The findings of A-MCF film presented specific capacitance of 401.4 F/g and rate capability of 336.2 F/g at a current density of 1 A/g and 1000 A/g respectively with 99.0% of capacitance retention after 20,000 cycles at 100 A/g as shown through

Figure 10. Despite this study lacks in controlling the pore size distribution and porosity as it is crucial for achieving optimal performance. The paper does not discuss the systematic control over the pore structure, which is vital for ensuring uniform ion diffusion and maximizing the surface area for charge storage.

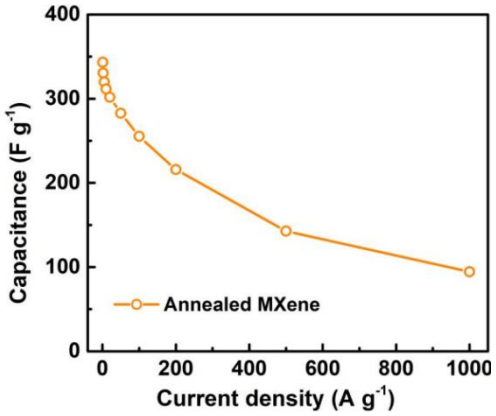

Figure 10. Rate capability of the annealed MXene film [99].

To further enhance the super capacitive results of $Ti_3C_2T_x$/CNTs, the incorporation of third element, including conducting polymers such as polypyrrole (PPy) or polyaniline (PANI), has been performed. For illustration, it has been seen that a theoretical specific capacitance of 400F/g has been presented by PANI in sulphuric acid. A few years back, Cai et al. [105] showed the preparation of $Ti_3C_2T_x$-CNT/PANI nanocomposite in one of their research projects. It has been revealed by SEM images that the composite of CNT/PANI built a strong connection with MXene ($Ti_3C_2T_x$) nanosheets, with a considerable positive effect on the stacking of $Ti_3C_2T_x$ sheets which improves the overall performance of energy storage devices. Compared with EDLC capacitance derived for MXene, the behavior reflected by the composition of $Ti_3C_2T_x$-CNT/PANI and CNT/PANI composites is pseudocapacitive with quasi-symmetrical curves which are because of the presence of redox active sites in PANI. Moreover, the capacitive reach of $Ti_3C_2T_x$-CNT/PANI electrode was 429.4 F/g under 1 M solution of H_2SO_4 at a current density of 1 A/g. This ternary composition of electrode materials proved excellent stability with 93% of capacitance retention after 10,000 cycles, higher than any of the single compound in the composite material.

An optimization of 3D interconnected structure of ion-permeable MXene/graphene nanotube (MG) composite film was carried by Wang et al. [106] through the insertion of graphene nanotubes (GDY-NTs) vertically into MXene ($Ti_3C_2T_x$) layers as shown in **Figure 11**. The representation of GDY-NTs was recognized as a latest artificially synthesized carbon allotrope, which delivered a synergistic effect because of horizontal-vertical 3D-intercalation thus improving the performance of MG films.

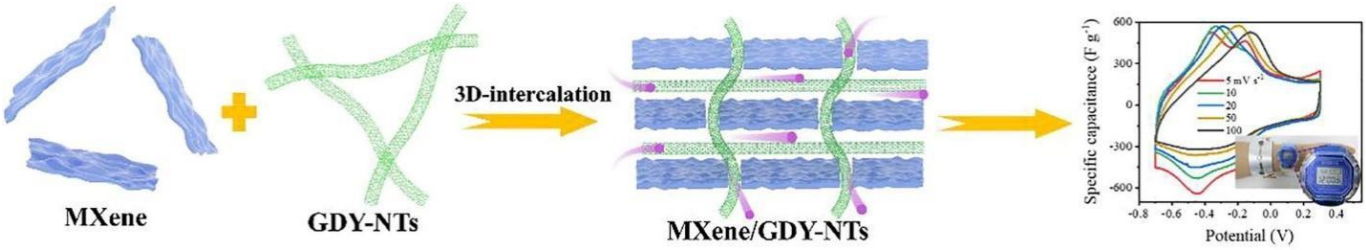

Figure 11. Capacitive effects of Intercalating GDY-NTs in MXene thin films.

In this discovery, it has been shown that the capacitance and the rate capacity delivered by this composite film has significantly improved to 337.4 F/g and 73% at 100 mV/s, which was higher than bare MXene ($Ti_3C_2T_x$) film. Hence, this research points towards a latest method in dealing with the problem of restacking in $Ti_3C_2T_x$ for SCs applications. However, as the synthesis of graphdiyne requires the need of organic solvents and precursors, it poses a strong impact on environmental if carefully not monitored which thus needs to be considered.

3.2.2. Investigating $Ti_3C_2T_X$/carbon nanofiber composites

Several benefits are offered by CNFs because of their easy fabrication methods and property to be used as self-standing electrodes for flexible SCs without requiring polymer binders or metal current collectors [107]. In general, on large scale, the flexibility in size and 1D morphology of CNFs can be obtained by carbonizing polymer precursors such as polyacrylonitrile (PAN), polyimide, polyvinyl alcohol, and aromatic polyamide [97]. By forming the composites of CNFs with MXene, properties of individual materials including their tendency of electrical conductivity and surface functionality got enhanced, thus preventing the issues of re-deposition and auto-oxidation in MXene.

It was portrayed by Kwon et al. [56] in their research about the synthesis of hybrid carbon nanofibers (HCNFs) prepared from $Ti_3C_2T_x$ and aromatic poly (ether amide) (PEA) for using as free-standing supercapacitor electrodes. The method involved spinning PEA solutions electrically and then these fibers are dip-coated for 1–10 cycles in $Ti_3C_2T_x$ aqueous solution Afterwards, $Ti_3C_2T_x$-coated PEA nanofibers were carbonized at a temperature of 1000 ℃. It is evaluated from the results that as the number of dips increases, MXene nanosheets spread uniformly on the entire PEA-derived and nitrogen-self-doped CNFs. After seven cycles of dip-coating, HCNF7 was produced successfully which delivered excellent values of electrochemical performance due to the balance between high conductivity and ionic barrier function of $Ti_3C_2T_x$/CNFs composite. The designed SC with two independent and symmetrical HCNF7 electrodes displayed prominent improvement in the electrochemical performance parameters with specific capacitance value ranging from 66.7 F/g to 179.3 F/g, power density from 1000 W/Kg to 10,000 W/Kg, along with the energy density from 52.7 Wh/Kg to 91.2 Wh/Kg at a current density ranging from 1 to 10 A/g. Thus, these $Ti_3C_2T_x$/PEA-derived HCNFs confirms to have the capability of portraying as high-performance self-standing electrode materials. Thereafter, a similar method was devised by Levitt et al. [99] for designing free-standing $Ti_3C_2T_x$/CNF electrodes by spinning $Ti_3C_2T_x$ electrically with PAN followed by carbonization. The weight ratio of mixing MXene flakes with PAN solutions was 1:2 (PAN:MXene), due

to which the percentage of MXene fiber mats prepared was 35 wt.%. The resulting hybrid film possessed capacitance of 205 mF/cm^2 at a scan rate of 50 mV/s, which was approximately three times greater than pure carbonized PAN nanofibers and twice by bare MXene ($Ti_3C_2T_x$) fibers.

Kshetri et al. [108] employed a rational concept of designing cobalt metal-organic framework (Co-MOF) on flexible conducting MXene-carbon nanofiber mats (MX-CNF). The composites of above said material were then used as the initial material for deriving capacitive-type Co-PC@MX-CNF and battery-type MnO_2@Co_3O_4-PC@MX-CNF individual electrodes for high-performance flexible and wearable hybrid SCs (FW-HSCs). Results show that the fabricated electrodes provide a specific capacitance of 426.7 F/g with a specific capacity of 475.4 mAh/g at 1 A/g. Moreover, fabricated FW-HSC achieved an energy density of 72.5 Wh/kg at a power density of 832.4 W/kg, with capacitance retention of 90.36% for over 10,000 cycles. These results thus proved FW-HSC electrodes as an efficient source for various wearable devices.

3.3. Investigating 2D graphene/$Ti_3C_2T_X$ composites

Graphene, a 2D family candidate composed of carbon layers with single atom thickness, displaying distinct characteristics than zero- and one-dimensional carbon materials as they involve a strong in-plane covalent bonding which provides excellent electrical conductivity, suitable layer thickness, wider lateral dimensions which shortens pathways for ion transport, and larger surface exposure which helps in adsorbing ions [109]. All these properties highly affect the performance of SCs [110]. Functionalized graphene's, such as porous, heteroatom-doped, hydrogels, and aerogels, have been widely explored in SCs. The surface groups behave as the redox sites on functionalized graphene, thus leading to their pseudocapacitive behavior [111]. While drying and fabricating electrode material, it's been observed that van der Waals forces interaction among nanosheets results in the problem of aggregation and self-restacking in graphene as well [109]. It is very interesting to note that when graphene material is introduced into MXene using self-assembly methods or other routes, it will remove the chances of self-stacking of individual materials and combines the benefits which each component carries for resulting high electrochemical capacitance [112].

The preparation of flexible MXene ($Ti_3C_2T_x$/holey graphene (MX-rHGO)) membranes were proposed by Fan et al. [113] by filtering the dispersions of alkalized $Ti_3C_2T_x$ and holey graphene oxide (HGO), in continuation with mild annealing treatment as shown in **Figure 12**. The outcomes of this study reveal that the porosity in graphene acted as a spacer for preventing self-stacking in $Ti_3C_2T_x$, thus building a strong network by connecting nanopores which facilitated the ion transport and shortening transport path for electrolyte ions.

From the results, it was shown that the gravimetric capacitance shown by MX-rHGO$_3$ film with 3 wt.% of holey graphene, displayed capacitance of 438 F/g at a scan rate of 2 mV/s, which was greater than pristine $Ti_3C_2T_x$ film (303 F/g) as presented in **Figure 13**. Moreover, with MX-rHGO$_3$ hybrid film, the value of bulk capacitance achieved was 1445 F/cm^3 at a scan rate of 2 mV/s with a capacitance retention of 69%

at 500 mV/s. Moreover, the with the use of MX-rHGO$_3$ film, symmetrical SC fabricated displayed a capacitance retention of 93% at 5 A/g for 10,000 cycles and showed an energy density of 38.6 Wh/L with a power density of 206 W/L.

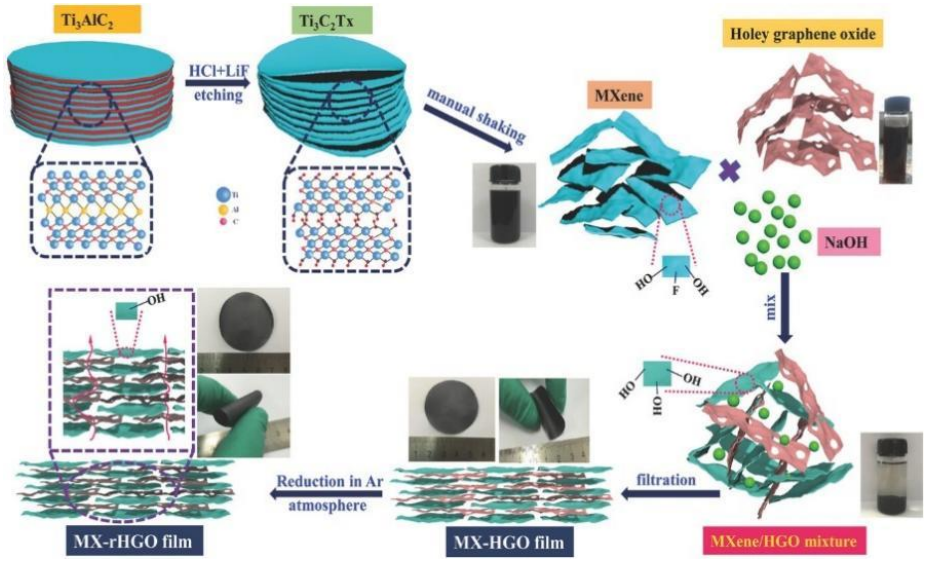

Figure 12. Illustration of synthesis of the modified MXene/holey graphene film.

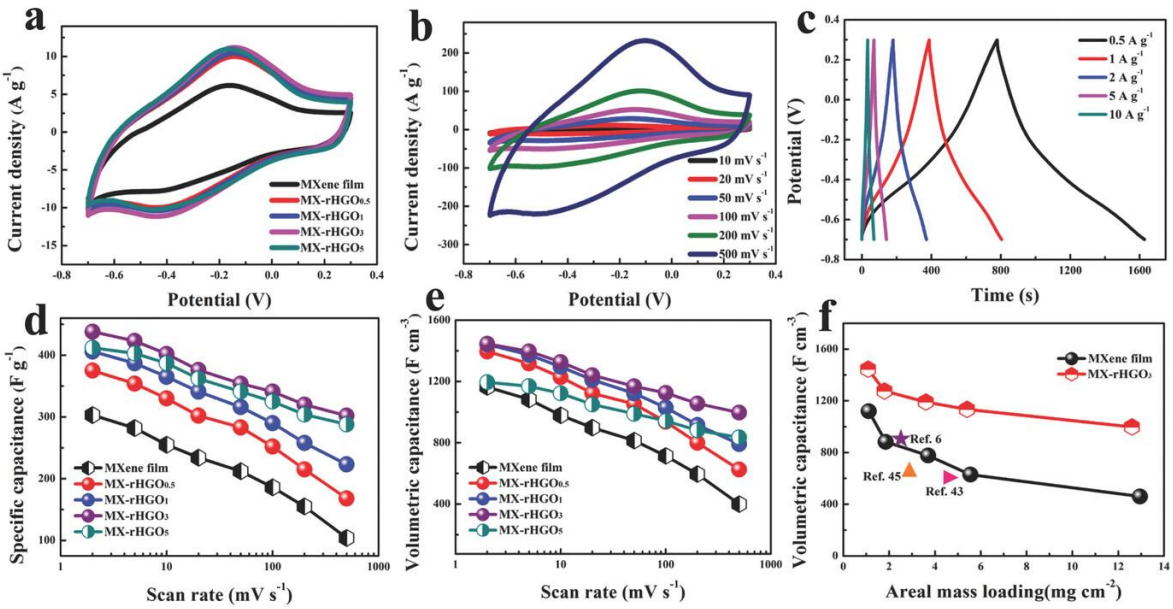

Figure 13. (a) Cyclic voltammetry curves of MXene film and MX-rHGO at a scan rate of 20 mV/s; **(b)** CV curves of MX-rHGO$_3$ at scan rates ranging from 10 to 500 mV/s; **(c)** constant current charge–discharge curves of MX-rHGO$_3$ at different current densities; **(d)** gravimetric and **(e)** volumetric capacitances of the MXene and MX-rHGO at different scan rates; **(f)** effect of areal mass loading on the volumetric capacitance of MXene film and MX-rHGO$_3$ in comparison with some previous reports.

Shao et al. [114] developed a hybrid aerogels of $Ti_3C_2T_x$/reduced graphene oxide (rGO) using a simple self-assembly method. The strong forces were shown by 3D porous aerogel in different directions with a unique spindle shape and stiffer pore walls. These aerogels displayed an electrochemical capacitance of 233 F/g at a current density of 1 A/g, along with a capacitive retention of 91.01% after 10,000 cycles. This

technique thus acts as a useful theoretical reference for carrying research on independent supercapacitor electrode materials.

A demonstration was conducted by Yan et al. [115] using electrostatic self-assembling method on $Ti_3C_2T_x$/rGO membranes which were highly flexible and conductive. In this method negatively charged nanosheets of MXene and positively charged nanosheets of reduced graphene oxide were assembled for creating rapid supercapacitor materials. This composite material results in minimizing the concern of self-restacking of rGO and $Ti_3C_2T_x$ nanosheets while maintaining the ultrahigh conductivity of 2261 S/cm and density of 3.1 g/cm^3. The rGO nanosheets acted as conductive spacers between MXene ($Ti_3C_2T_x$) with an increase in its interlayer spacing for creating various channels for electrolyte ions as shown through SEM images in **Figure 14**. Thus, the synthesized M/G-5% electrode provided a specific capacitance of 335.4 F/g at a scan rate of 2 mV/s, which was slightly greater than pure MXene (330.2 F/g). Furthermore, results have also shown that there was no degradation of capacitance value even after 20,000 cycles.

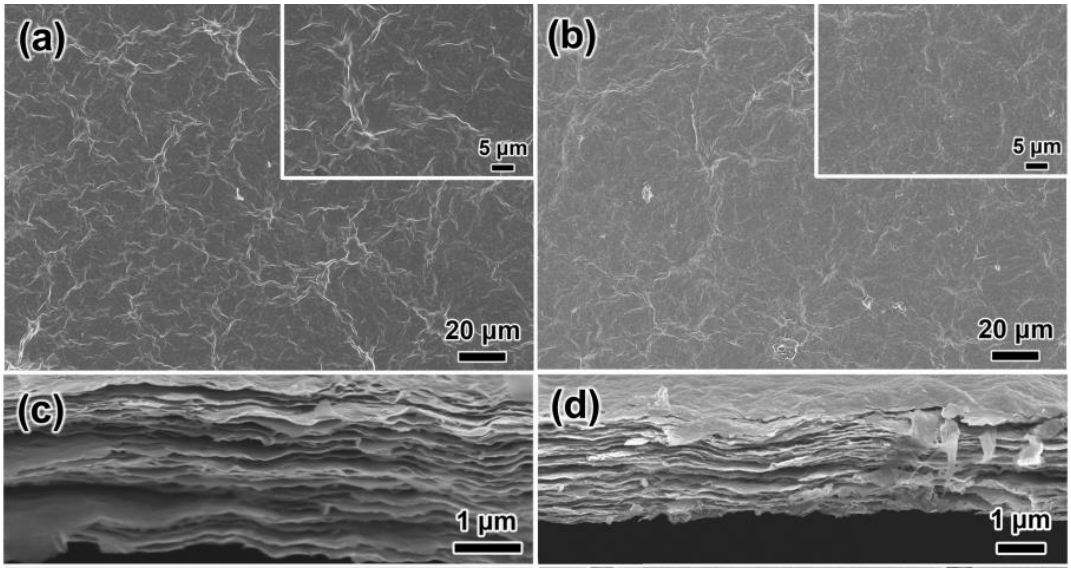

Figure 14. (a) and **(b)** Top-view; **(c)** and **(d)** cross-sectional SEM images of the resultant of M/G-1%; **(a)** and **(c)** M/G-10%; **(b)** and **(d)**, insets are the high-magnification SEM images.

Later, a study by Yang et al. [116] presented an efficient and fast self- assembly method for preparing 3-dimensional porous antioxidant $Ti_3C_2T_x$/graphene (PMG) hybrid with the help of in-situ killed metal zinc templates. This self-assembled porous 3D structure mitigated the concerns of oxidation in MXene and exhibited outstanding conductivity due to the accessibility of redox active sites by electrolyte ions. The SEM results for the PMG-5 is shown through **Figure 15**. The synthesized hybrid PMG-5 electrode (having 5% rGO content) resulted in an outstanding specific capacitance of 393 F/g, and excellent cycling stability. Additionally, the fabricated asymmetrical supercapacitor displayed an energy density of 50.8 Wh/kg with a 4.3% decrease in the value of capacitance after capacitive cycles of 10,000.

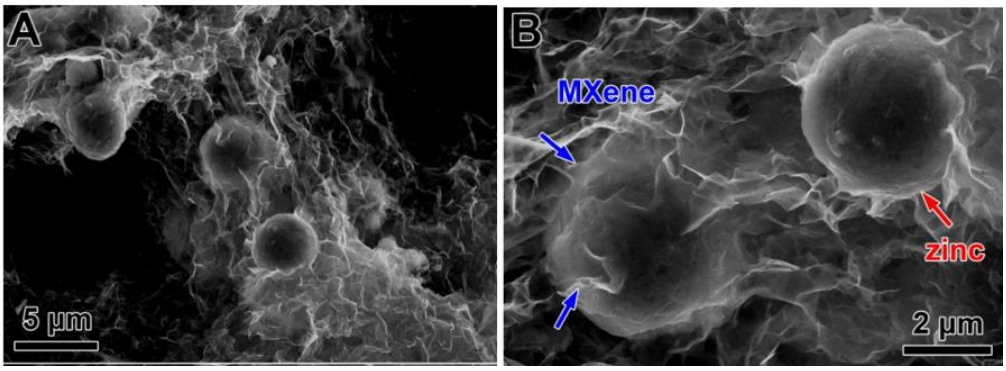

Figure 15. SEM images. **(A)** and **(B)** PMG-5 sample without the removal of zinc powder by concentrated HCl solution.

This work gives insights into a new strategy for tackling two significant long-term issues faced by $Ti_3C_2T_x$ in future. Despite of only combining MXene and graphene materials for eliminating the problem of self-stacking there are other strategies too such as surface modification or ligand-assisted routes that also needs to be used for solving the issues of self-stacking. Further, the process of graphene synthesis is also tedious needs and consume high energy with low output [102]. Thus, there is still a gap left for improving its production efficiency with minimizing the cost of its production.

3.4. Investigating 3D carbon/$Ti_3C_2T_X$ composites

3D carbon materials have interconnection of porous structure which leads to high electrical conductivity, faster ion transfer dynamics, and greater redox active surface area [117]. With the smaller 3D materials, their incorporation into different layers of MXene is easy comparatively to the insertion of larger 3D materials. In this section, the introduction of combining 3D carbons with MXene $Ti_3C_2T_x$ is discussed thoroughly including the benefits shown by their combination in supercapacitors.

3.4.1. Activated carbon (AC)

The cost effectiveness as well as the porosity tunability makes AC a most used candidate for supercapacitors. Yu et al. [118] reported in their research about single-step synthesis of $Ti_3C_2T_x$/AC composite as electrodes for flexible SCs with organic electrolyte. It can be seen from the findings of this publication that AC particles were incorporated among MXene ($Ti_3C_2T_x$) layers in which the role of binders, conductive additives and flexibility is provided by MXenes. Due to AC encapsulation, the interlayer distance between MXene layers is expanded which improved the specific capacitance and stability of electrodes as depicted through XRD pattern with the shifting of peak at 9.5 degrees to lower value in **Figure 16**. The results showed that the flexible MXene/AC hybrid electrode displayed a capacitance of value 126 F/g at a current density of 0.1 A/g, with a capacitive retention of 92.4% after 10,000 cycles at 10 A/g.

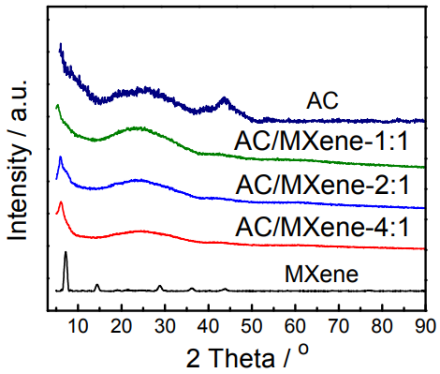

Figure 16. XRD patterns of AC particles, MXene film, and AC/MXene films.

3.4.2. MOF-derived carbon

The formation of MOFs is carried out with the help of coordination reaction occurring between metal-containing units and organic linkers. Because of the variable metal ions, rich carbon content, and excellent pore structure, porous carbon-based materials are prepared by utilizing MOFs as precursor material [82]. In a study recently adopted by Gao et al. [119] displayed the preparation of mesoporous carbon (MCs) using carbonizing zeolite imidazole framework-8 (gaoZIF-8) as a precursor material, which presented a capacitance of 215 F/g. Later, Jiang et al. [120] carried another research for developing in-situ decorated ZIF-67 nanoparticles on 2D ultrathin Ti_3C_2 nanosheets followed by calcination at 800 ℃ in the atmosphere of hydrogen and argon for 2 h along with the removal of metal ions via acid treatment as shown in **Figure 17**. During the process of carbonization, ZIF-67 acted as a source of nitrogen provider for carrying out doping in Ti_3C_2. Therefore, the hybrid nitrogen-doped Ti_3C_2/carbon 2D heterostructure (N-Ti_3C_2/C) was finally achieved, which can be a diaphragm for lithium-sulfur batteries and had wide range of possibilities to be used in coming years in SCs.

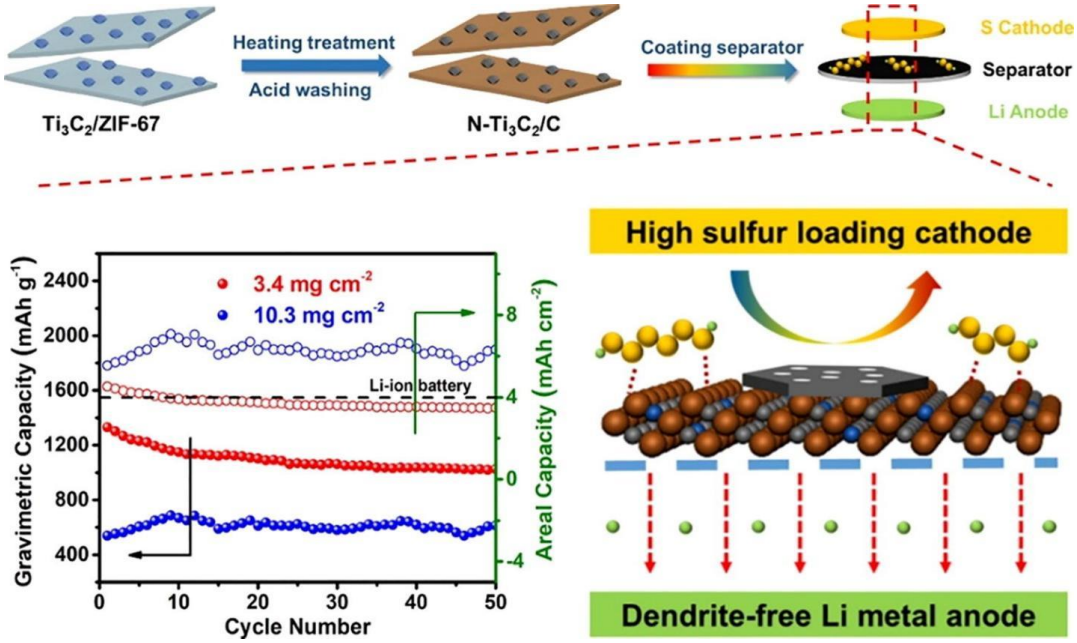

Figure 17. Synthesis process of $Ti_3C_2T_x$/ZIF-67 composite electrodes.

4. Summary and perspectives

MXene belongs to an emerging class of two-dimensional transition metal carbides or nitrides which shows outstanding results for different energy storage applications. Thie 2D layered structure possesses attractive density, excellent electron conductivity, better hydrophilicity, variable terminations, and mechanism of charge storage via ions intercalation. This paper mainly aims towards popularly used modification and widely used methods for the successful synthesis of MXene ($Ti_3C_2T_x$) with varied sized of carbon materials in the field of supercapacitors. Firstly, this paper starts with introducing different synthesis methods of MXene, such as HF etching, acid/fluoride etching, alkali etching, molten salt etching, electrochemical etching, etc. All these methods have serious effect on different parameters of MXene including functional groups, sheet size and interlayer spacing, and its final electrochemical properties with different composites. Secondly, for mitigating the problem of restacking and oxidation in MXene, they are utilized either as active material or additive or host, or as a substrate for 0D, 1D, 2D, 3D carbon as this can help in exposing the surface accessibility of MXene. The output with 0-dimensional carbon derivatives showed that these have possesses higher active sites, and larger specific surface areas. Moreover, the enhancement in rate capabilities can be achieved by employing 1D carbon materials because of large conductive networks and convenient channels for faster ion and electron transport, whereas the improvement in electrical conductivity is provided by 2D materials. Moreover, benefits of bigger lateral 2D dimensions can be easily applied for improving the specific capacitance and stability of the corresponding supercapacitors. In addition, 3D materials with wide exposure surfaces and flexible porous structures proves them as an ideal electrode material for high-performance SC applications. However, although big achievements are remarked by designing MXene/carbon composites in SC applications, still there are various challenges and possibilities for the upcoming future. In summary, there are few factors which needs to be addressed for future growth as (i) sustainable methods for preparation of $Ti_3C_2T_x$; (ii) design improvement of MXenes/carbon hybrids; (iii) practical applications development on MXene-based SCs. In-depth research on all the above-mentioned aspects can be promoted for the further development of MXene/carbon hybrids as high-performance SC materials.

Conflict of interest: The author declares no conflict of interest.

References

1. Verma S, Arya S, Gupta V, et al. Performance analysis, challenges and future perspectives of nickel based nanostructured electrodes for electrochemical supercapacitors. Journal of Materials Research and Technology. 2021; 11: 564–599. doi: 10.1016/j.jmrt.2021.01.027
2. Miao L, Song Z, Zhu D, et al. Recent advances in carbon-based supercapacitors. Materials Advances. 2020; 1(5): 945–966. doi: 10.1039/d0ma00384k
3. Huang J, Lu X, Sun T, et al. Boosting High-Voltage Dynamics Towards High-Energy-Density Lithium-Ion Capacitors. Energy & Environmental Materials. 2023; 6(4). doi: 10.1002/eem2.12505
4. Wei C, Fei H, Tian Y, et al. Isotropic Li nucleation and growth achieved by an amorphous liquid metal nucleation seed on MXene framework for dendrite-free Li metal anode. Energy Storage Materials. 2020; 26: 223–233. doi: 10.1016/j.ensm.2020.01.005

5. Wei C, Xi B, Wang P, et al. In Situ Anchoring Ultrafine ZnS Nanodots on 2D MXene Nanosheets for Accelerating Polysulfide Redox and Regulating Li Plating. Advanced Materials. 2023; 35(32). doi: 10.1002/adma.202303780
6. Ding J, He D, Du P, et al. Design Photocatalysts to Boost Carrier Dynamics in Plastics Photoconversion into Fuels. ACS Applied Materials & Interfaces. 2024; 16(28): 35865-35873. doi: 10.1021/acsami.4c07664
7. N RY, Sharma K, Shafi PM. An overview, methods of synthesis and modification of carbon-based electrodes for supercapacitor. Journal of Energy Storage. 2022; 55: 105727. doi: 10.1016/j.est.2022.105727
8. Raj B, Padhy A, Basu S, et al. Review—Futuristic Direction for R&D Challenges to Develop 2D Advanced Materials Based Supercapacitors. Journal of The Electrochemical Society. 2020; 167(13): 136501. doi: 10.1149/1945-7111/abb40d
9. Jiang Q, Kurra N, Alhabeb M, et al. All Pseudocapacitive MXene-RuO2 Asymmetric Supercapacitors. Advanced Energy Materials. 2018; 8(13). doi: 10.1002/aenm.201703043
10. Wang Y, Chu X, Zhang H, et al. Hyper-conjugated polyaniline delivering extraordinary electrical and electrochemical properties in supercapacitors. Applied Surface Science. 2023; 628: 157350. doi: 10.1016/j.apsusc.2023.157350
11. Abbas Q, Mirzaeian M, Hunt MRC, et al. Current State and Future Prospects for Electrochemical Energy Storage and Conversion Systems. Energies. 2020; 13(21): 5847. doi: 10.3390/en13215847
12. Navarro G, Torres J, Blanco M, et al. Present and Future of Supercapacitor Technology Applied to Powertrains, Renewable Generation and Grid Connection Applications. Energies. 2021; 14(11): 3060. doi: 10.3390/en14113060
13. Khalid M. A Review on the Selected Applications of Battery-Supercapacitor Hybrid Energy Storage Systems for Microgrids. Energies. 2019; 12(23): 4559. doi: 10.3390/en12234559
14. Kasprzak D, Mayorga-Martinez CC, Pumera M. Sustainable and Flexible Energy Storage Devices: A Review. Energy & Fuels. 2022; 37(1): 74–97. doi: 10.1021/acs.energyfuels.2c03217
15. Shao Y, El-Kady MF, Sun J, et al. Design and Mechanisms of Asymmetric Supercapacitors. Chemical Reviews. 2018; 118(18): 9233–9280. doi: 10.1021/acs.chemrev.8b00252
16. Garg R, Agarwal A, Agarwal M. A review on MXene for energy storage application: effect of interlayer distance. Materials Research Express. 2020; 7(2): 022001. doi: 10.1088/2053-1591/ab750d
17. Zhai Z, Zhang L, Du T, et al. A review of carbon materials for supercapacitors. Materials & Design. 2022; 221: 111017. doi: 10.1016/j.matdes.2022.111017
18. Zhou Q, Yao H. Recent development of carbon electrode materials for electrochemical supercapacitors. Energy Reports. 2022; 8: 656–661. doi: 10.1016/j.egyr.2022.09.167
19. Simon P, Gogotsi Y. Materials for electrochemical capacitors. Nature Materials. 2008; 7(11): 845–854. doi: 10.1038/nmat2297
20. Boota M, Gogotsi Y. MXene—Conducting Polymer Asymmetric Pseudocapacitors. Advanced Energy Materials. 2018; 9(7). doi: 10.1002/aenm.201802917
21. Gan Z, Yin J, Xu X, et al. Nanostructure and advanced energy storage: elaborate material designs lead to high-rate pseudocapacitive ion storage. ACS Nano. 2022; 16(4): 5131–5152.
22. Jiang X, Chu X, Zhang X, et al. Surplus charge injection enables high-cell-potential stable 2D polyaniline supercapacitors. Electrochim Acta. 2023; 445: 142052.
23. Garg R, Agarwal A, Agarwal M. Performance of copper sulfide hollow rods in a supercapacitor based on flexible substrates. Journal of Electronic Materials. 2021; 50: 6974–6980.
24. Kumar S, Saeed G, Zhu L, et al. 0D to 3D carbon-based networks combined with pseudocapacitive electrode material for high energy density supercapacitor: a review. Chemical Engineering Journal. 2021; 403: 126352.
25. Jiang Y, Liu J. Definitions of pseudocapacitive materials: a brief review. Energy & Environmental Materials. 2019; 2(1): 30–37.
26. Liu Y, Jiang SP, Shao Z. Intercalation pseudocapacitance in electrochemical energy storage: recent advances in fundamental understanding and materials development. Materials Today Advances. 2020; 7: 100072. doi: 10.1016/j.mtadv.2020.100072
27. Li J, Wang H, Xiao X. Intercalation in Two-Dimensional Transition Metal Carbides and Nitrides (MXenes) toward Electrochemical Capacitor and Beyond. Energy & Environmental Materials. 2020; 3(3): 306–322. doi: 10.1002/eem2.12090
28. Muzaffar A, Ahamed MB, Deshmukh K, et al. A review on recent advances in hybrid supercapacitors: Design, fabrication and applications. Renewable and Sustainable Energy Reviews. 2019; 101: 123–145. doi: 10.1016/j.rser.2018.10.026
29. Zuo W, Li R, Zhou C, et al. Battery-Supercapacitor Hybrid Devices: Recent Progress and Future Prospects. Advanced Science. 2017; 4(7). doi: 10.1002/advs.201600539

30. Shi Y, Liu G, Jin R, et al. Carbon materials from melamine sponges for supercapacitors and lithium battery electrode materials: A review. Carbon Energy. 2019; 1(2): 253–275. doi: 10.1002/cey2.19
31. Huang S, Zhu X, Sarkar S, et al. Challenges and opportunities for supercapacitors. APL Materials. 2019; 7(10). doi: 10.1063/1.5116146
32. Baig MM, Gul IH, Baig SM, et al. 2D MXenes: Synthesis, properties, and electrochemical energy storage for supercapacitors—A review. Journal of Electroanalytical Chemistry. 2022; 904: 115920. doi: 10.1016/j.jelechem.2021.115920
33. Garg R, Agarwal A, Agarwal M. Effect of vanadium doping on MXene-based supercapacitor. Journal of Materials Science: Materials in Electronics. 2021; 32(17): 22046–22059. doi: 10.1007/s10854-021-06668-x
34. Venkateshalu S, Grace AN. MXenes—A new class of 2D layered materials: Synthesis, properties, applications as supercapacitor electrode and beyond. Applied Materials Today. 2020; 18: 100509. doi: 10.1016/j.apmt.2019.100509
35. Zhu Q, Li J, Simon P, et al. Two-dimensional MXenes for electrochemical capacitor applications: Progress, challenges and perspectives. Energy Storage Materials. 2021; 35: 630–660. doi: 10.1016/j.ensm.2020.11.035
36. Wang Y, Wang Y. Recent progress in MXene layers materials for supercapacitors: High-performance electrodes. SmartMat. 2022; 4(1). doi: 10.1002/smm2.1130
37. Wei Y, Zhang P, Soomro RA, et al. Advances in the Synthesis of 2D MXenes. Advanced Materials. 2021; 33(39). doi: 10.1002/adma.202103148
38. Garg R, Agarwal M. MXene: A new revolution in the world of 2-D materials. Energy Storage and Conversion. 2024; 2(4): 1613. doi: 10.59400/esc1613
39. Wang Z, Xu Z, Huang H, et al. Unraveling and Regulating Self-Discharge Behavior of Ti3C2Tx MXene-Based Supercapacitors. ACS Nano. 2020; 14(4): 4916–4924. doi: 10.1021/acsnano.0c01056
40. Wei C, Tao Y, An Y, et al. Recent Advances of Emerging 2D MXene for Stable and Dendrite-Free Metal Anodes. Advanced Functional Materials. 2020; 30(45). doi: 10.1002/adfm.202004613
41. Zhang C, Ma Y, Zhang X, et al. Two-Dimensional Transition Metal Carbides and Nitrides (MXenes): Synthesis, Properties, and Electrochemical Energy Storage Applications. Energy & Environmental Materials. 2019; 3(1): 29–55. doi: 10.1002/eem2.12058
42. Chen Y, Yang H, Han Z, et al. MXene-Based Electrodes for Supercapacitor Energy Storage. Energy & Fuels. 2022; 36(5): 2390–2406. doi: 10.1021/acs.energyfuels.1c04104
43. Gogotsi Y, Huang Q. MXenes: Two-Dimensional Building Blocks for Future Materials and Devices. ACS Nano. 2021; 15(4): 5775–5780. doi: 10.1021/acsnano.1c03161
44. Jiang X, Wu X, Xie Y, et al. Additive Engineering Enables Ionic-Liquid Electrolyte-Based Supercapacitors to Deliver Simultaneously High Energy and Power Density. ACS Sustainable Chemistry & Engineering. 2023; 11(14): 5685–5695. doi: 10.1021/acssuschemeng.3c00213
45. Tian Y, Yang C, Luo Y, et al. Understanding MXene-Based "Symmetric" Supercapacitors and Redox Electrolyte Energy Storage. ACS Applied Energy Materials. 2020; 3(5): 5006–5014. doi: 10.1021/acsaem.0c00527
46. Tang X, Guo X, Wu W, et al. 2D Metal Carbides and Nitrides (MXenes) as High-Performance Electrode Materials for Lithium-Based Batteries. Advanced Energy Materials. 2018; 8(33). doi: 10.1002/aenm.201801897
47. Naguib M, Mochalin VN, Barsoum MW, et al. 25th Anniversary Article: MXenes: A New Family of Two-Dimensional Materials. Advanced Materials. 2013; 26(7): 992–1005. doi: 10.1002/adma.201304138
48. Feng A, Yu Y, Wang Y, et al. Two-dimensional MXene Ti3C2 produced by exfoliation of Ti3AlC2. Materials & Design. 2017; 114: 161–166. doi: 10.1016/j.matdes.2016.10.053
49. Li Y, Deng Y, Zhang J, et al. Tunable energy storage capacity of two-dimensional Ti3C2Txmodified by a facile two-step pillaring strategy for high performance supercapacitor electrodes. Nanoscale. 2019; 11(45): 21981–21989. doi: 10.1039/c9nr07259d
50. Ajmal Z, Qadeer A, Khan U, et al. Current progresses in two-dimensional MXene-based framework: prospects from superficial synthesis to energy conversion and storage applications. Materials Today Chemistry. 2023; 27: 101238. doi: 10.1016/j.mtchem.2022.101238
51. Huang H, He J, Wang Z, et al. Scalable, and low-cost treating-cutting-coating manufacture platform for MXene-based on-chip micro-supercapacitors. Nano Energy. 2020; 69: 104431. doi: 10.1016/j.nanoen.2019.104431
52. Pu S, Wang Z, Xie Y, et al. Origin and Regulation of Self-Discharge in MXene Supercapacitors. Advanced Functional Materials. 2022; 33(8). doi: 10.1002/adfm.202208715

53. Gogotsi Y, Anasori B. The Rise of MXenes. ACS Nano. 2019; 13(8): 8491–8494. doi: 10.1021/acsnano.9b06394
54. Zhang Y, Feng Z, Wang X, et al. MXene/carbon composites for electrochemical energy storage and conversion. Materials Today Sustainability. 2023; 22: 100350. doi: 10.1016/j.mtsust.2023.100350
55. Elemike EE, Adeyemi J, Onwudiwe DC, et al. The future of energy materials: A case of MXenes-carbon dots nanocomposites. Journal of Energy Storage. 2022; 50: 104711. doi: 10.1016/j.est.2022.104711
56. Kwon YS, Lee J, Hwang G, et al. Hybrid Carbon Nanofibers Derived from MXene Nanosheets and Aromatic Poly (ether amide) for Self-Standing Electrochemical Energy Storage Materials. Macromolecular Materials and Engineering. 2022; 307(5). doi: 10.1002/mame.202100877
57. Garg R, Agarwal A, Agarwal M. Synthesis and optimisation of MXene for supercapacitor application. Journal of Materials Science: Materials in Electronics. 2020; 31(21): 18614–18626. doi: 10.1007/s10854-020-04404-5
58. Lin Z, Shao H, Xu K, et al. MXenes as High-Rate Electrodes for Energy Storage. Trends in Chemistry. 2020; 2(7): 654–664. doi: 10.1016/j.trechm.2020.04.010
59. Lu M, Zhang Z, Kang L, et al. Intercalation and delamination behavior of Ti3C2Txand MnO2/Ti3C2Tx/RGO flexible fibers with high volumetric capacitance. Journal of Materials Chemistry A. 2019; 7(20): 12582–12592. doi: 10.1039/c9ta01993f
60. Fu Q, Wen J, Zhang N, et al. Free-standing Ti3C2Txelectrode with ultrahigh volumetric capacitance. RSC Advances. 2017; 7(20): 11998–12005. doi: 10.1039/c7ra00126f
61. Ferrara C, Gentile A, Marchionna S, et al. $Ti_3C_2T_x$ MXene compounds for electrochemical energy storage. Current Opinion in Electrochemistry. 2021; 29: 100764. doi: 10.1016/j.coelec.2021.100764
62. Forouzandeh P, Pillai SC. MXenes-based nanocomposites for supercapacitor applications. Current Opinion in Chemical Engineering. 2021; 33: 100710. doi: 10.1016/j.coche.2021.100710
63. Garg R, Agarwal A, Agarwal M. Synthesis and characterization of solution processed MXene. DAE Solid State Physics Symposium 2019. 2020; 2265: 030665. doi: 10.1063/5.0016599
64. Naguib M, Kurtoglu M, Presser V, et al. Two-Dimensional Nanocrystals Produced by Exfoliation of Ti3AlC2. Advanced Materials. 2011; 23(37): 4248–4253. doi: 10.1002/adma.201102306
65. Naguib M, Mashtalir O, Carle J, et al. Two-Dimensional Transition Metal Carbides. ACS Nano. 2012; 6(2): 1322–1331. doi: 10.1021/nn204153h
66. Ghidiu M, Lukatskaya MR, Zhao MQ, et al. Conductive two-dimensional titanium carbide 'clay' with high volumetric capacitance. Nature. 2014; 516(7529): 78–81. doi: 10.1038/nature13970
67. Barsoum MW, Radovic M. Elastic and Mechanical Properties of the MAX Phases. Annual Review of Materials Research. 2011; 41(1): 195–227. doi: 10.1146/annurev-matsci-062910-100448
68. Lukatskaya MR, Mashtalir O, Ren CE, et al. Cation Intercalation and High Volumetric Capacitance of Two-Dimensional Titanium Carbide. Science. 2013; 341(6153): 1502–1505. doi: 10.1126/science.1241488
69. Xie X, Xue Y, Li L, et al. Surface Al leached Ti_3AlC_2 as a substitute for carbon for use as a catalyst support in a harsh corrosive electrochemical system. Nanoscale. 2014; 6(19): 11035–11040. doi: 10.1039/c4nr02080d
70. Dall' Agnese Y, Lukatskaya MR, Cook KM, et al. High capacitance of surface-modified 2D titanium carbide in acidic electrolyte. Electrochemistry Communications. 2014; 48: 118–122. doi: 10.1016/j.elecom.2014.09.002
71. Li J, Yuan X, Lin C, et al. Achieving High Pseudocapacitance of 2D Titanium Carbide (MXene) by Cation Intercalation and Surface Modification. Advanced Energy Materials. 2017; 7(15). doi: 10.1002/aenm.201602725
72. Li T, Yao L, Liu Q, et al. Fluorine-Free Synthesis of High-Purity Ti3C2Tx (T=OH, O) via Alkali Treatment. Angewandte Chemie International Edition. 2018; 57(21): 6115–6119. doi: 10.1002/anie.201800887
73. Lukatskaya MR, Kota S, Lin Z, et al. Ultra-high-rate pseudocapacitive energy storage in two-dimensional transition metal carbides. Nature Energy. 2017; 2(8). doi: 10.1038/nenergy.2017.105
74. Deng Y, Shang T, Wu Z, et al. Fast Gelation of $Ti_3C_2T_x$ MXene Initiated by Metal Ions. Advanced Materials. 2019; 31(43). doi: 10.1002/adma.201902432
75. Tang J, Mathis T, Zhong X, et al. Optimizing Ion Pathway in Titanium Carbide MXene for Practical High-Rate Supercapacitor. Advanced Energy Materials. 2020; 11(4). doi: 10.1002/aenm.202003025
76. Li M, Lu J, Luo K, et al. Element Replacement Approach by Reaction with Lewis Acidic Molten Salts to Synthesize Nanolaminated MAX Phases and MXenes. Journal of the American Chemical Society. 2019; 141(11): 4730–4737. doi: 10.1021/jacs.9b00574

77. Sun W, Shah SA, Chen Y, et al. Electrochemical etching of Ti_2AlC to Ti_2CT_x (MXene) in low-concentration hydrochloric acid solution. J Mater Chem A. 2017; 5(41): 21663–21668. doi: 10.1039/c7ta05574a
78. Shi CZY, Zhao D, et al. Iodide ion intercalation into MXene lattice towards energy storage applications. Nano Energy. 2018; 51: 9.
79. Yang S, Zhang P, Wang F, et al. Fluoride-Free Synthesis of Two-Dimensional Titanium Carbide (MXene) Using A Binary Aqueous System. Angewandte Chemie International Edition. 2018; 57(47): 15491–15495. doi: 10.1002/anie.201809662
80. Zhang S, Huang P, Wang J, et al. Fast and Universal Solution-Phase Flocculation Strategy for Scalable Synthesis of Various Few-Layered MXene Powders. The Journal of Physical Chemistry Letters. 2020; 11(4): 1247–1254. doi: 10.1021/acs.jpclett.9b03682
81. Zhao M, Ren CE, Ling Z, et al. Flexible MXene/Carbon Nanotube Composite Paper with High Volumetric Capacitance. Advanced Materials. 2014; 27(2): 339–345. doi: 10.1002/adma.201404140
82. Yu L, Hu L, Anasori B, et al. MXene-Bonded Activated Carbon as a Flexible Electrode for High-Performance Supercapacitors. ACS Energy Letters. 2018; 3(7): 1597–1603. doi: 10.1021/acsenergylett.8b00718
83. Bai T, Wang W, Xue G, et al. Free-Standing, Flexible Carbon@MXene Films with Cross-Linked Mesoporous Structures toward Supercapacitors and Pressure Sensors. ACS Applied Materials & Interfaces. 2021; 13(48): 57576–57587. doi: 10.1021/acsami.1c16589
84. Zhu C, Geng F. Macroscopic MXene ribbon with oriented sheet stacking for high-performance flexible supercapacitors. Carbon Energy. 2020; 3(1): 142–152. doi: 10.1002/cey2.65
85. Gu Q, Cao Y, Lu M, et al. MXene materials in electrochemical energy storage systems. Chemical Communications. 2024; 60(64): 8339–8349. doi: 10.1039/d4cc02659d
86. Chen M, Fan Q, Yu P, et al. Engineering Ti_3C_2-MXene Surface Composition for Excellent Li+ Storage Performance. Molecules. 2024; 29(8): 1731. doi: 10.3390/molecules29081731
87. Wang YQ, Zhang DT, Zhao B, et al. Ti_3C_2/Graphene Oxide Layered Nanocomposites for Enhanced Lithium-Ion Storage. ACS Applied Nano Materials. 2023; 6(5): 3572–3579. doi: 10.1021/acsanm.2c05298
88. Bhat VS, Toghan A, Hegde G, et al. Capacitive dominated charge storage in supermicropores of self-activated carbon electrodes for symmetric supercapacitors. Journal of Energy Storage. 2022; 52: 104776. doi: 10.1016/j.est.2022.104776
89. Zhu J, Yang D, Yin Z, et al. Graphene and Graphene-Based Materials for Energy Storage Applications. Small. 2014; 10(17): 3480–3498. doi: 10.1002/smll.201303202
90. Yuan M, Zhong R, Gao H, et al. One-step, green, and economic synthesis of water-soluble photoluminescent carbon dots by hydrothermal treatment of wheat straw, and their bio-applications in labeling, imaging, and sensing. Applied Surface Science. 2015; 355: 1136–1144. doi: 10.1016/j.apsusc.2015.07.095
91. Li L, Wu S, Wu K, et al. Carbon Dot-Regulated 2D MXene Films with High Volumetric Capacitance. Industrial & Engineering Chemistry Research. 2020; 59(31): 13969–13978. doi: 10.1021/acs.iecr.0c01440
92. Zhang P, Li J, Yang D, et al. Flexible Carbon Dots-Intercalated MXene Film Electrode with Outstanding Volumetric Performance for Supercapacitors. Advanced Functional Materials. 2022; 33(1). doi: 10.1002/adfm.202209918
93. Li Y, Liu J, Gong T, et al. One-step hydrothermal preparation of a novel 2D MXene-based composite electrode material synergistically modified by CuS and carbon dots for supercapacitors. Journal of Alloys and Compounds. 2023; 947: 169400. doi: 10.1016/j.jallcom.2023.169400
94. Tan Z, Wang W, Zhu M, et al. $Ti_3C_2T_x$ MXene@carbon dots hybrid microflowers as a binder-free electrode material toward high capacity capacitive deionization. Desalination. 2023; 548: 116267. doi: 10.1016/j.desal.2022.116267
95. Yang L, Zheng W, Zhang P, et al. MXene/CNTs films prepared by electrophoretic deposition for supercapacitor electrodes. Journal of Electroanalytical Chemistry. 2018; 830–831: 1–6. doi: 10.1016/j.jelechem.2018.10.024
96. Wang Z, Qin S, Seyedin S, et al. High-Performance Biscrolled MXene/Carbon Nanotube Yarn Supercapacitors. Small. 2018; 14(37). doi: 10.1002/smll.201802225
97. Nie G, Zhao X, Luan Y, et al. Key issues facing electrospun carbon nanofibers in energy applications: on-going approaches and challenges. Nanoscale. 2020; 12(25): 13225–13248. doi: 10.1039/d0nr03425h
98. Qin L, Yang D, Zhang M, et al. Superelastic and ultralight electrospun carbon nanofiber/MXene hybrid aerogels with anisotropic microchannels for pressure sensing and energy storage. Journal of Colloid and Interface Science. 2021; 589: 264–274. doi: 10.1016/j.jcis.2020.12.102

99. Yang X, Chen Y, Zhang C, et al. Electrospun carbon nanofibers and their reinforced composites: Preparation, modification, applications, and perspectives. Composites Part B: Engineering. 2023; 249: 110386. doi: 10.1016/j.compositesb.2022.110386
100. Zhang H, Su H, Zhang L, et al. Flexible supercapacitors with high areal capacitance based on hierarchical carbon tubular nanostructures. Journal of Power Sources. 2016; 331: 332–339. doi: 10.1016/j.jpowsour.2016.09.064
101. Moon RJ, Martini A, Nairn J, et al. Cellulose nanomaterials review: structure, properties and nanocomposites. Chemical Society Reviews. 2011; 40(7): 3941. doi: 10.1039/c0cs00108b
102. Zhou J, Zhang S, Zhou YN, et al. Biomass-Derived Carbon Materials for High-Performance Supercapacitors: Current Status and Perspective. Electrochemical Energy Reviews. 2021; 4(2): 219–248. doi: 10.1007/s41918-020-00090-3
103. Wang Q, Yuan H, Zhang M, et al. A Highly Conductive and Supercapacitive MXene/N-CNT Electrode Material Derived from a MXene-Co-Melamine Precursor. ACS Applied Electronic Materials. 2023; 5(5): 2506–2517. doi: 10.1021/acsaelm.2c01768
104. Li K, Zhang P, Soomro RA, et al. Alkali-Induced Porous MXene/Carbon Nanotube-Based Film Electrodes for Supercapacitors. ACS Applied Nano Materials. 2022; 5(3): 4180–4186. doi: 10.1021/acsanm.2c00109
105. Cai YZ, Fang YS, Cao WQ, et al. MXene-CNT/PANI ternary material with excellent supercapacitive performance driven by synergy. Journal of Alloys and Compounds. 2021; 868: 159159. doi: 10.1016/j.jallcom.2021.159159
106. Wang Y, Chen N, Liu Y, et al. MXene/Graphdiyne nanotube composite films for Free-Standing and flexible Solid-State supercapacitor. Chemical Engineering Journal. 2022; 450: 138398. doi: 10.1016/j.cej.2022.138398
107. Levitt AS, Alhabeb M, Hatter CB, et al. Electrospun MXene/carbon nanofibers as supercapacitor electrodes. Journal of Materials Chemistry A. 2019; 7(1): 269–277. doi: 10.1039/c8ta09810g
108. Kshetri T, Khumujam DD, Singh TI, et al. Co-MOF@MXene-carbon nanofiber-based freestanding electrodes for a flexible and wearable quasi-solid-state supercapacitor. Chemical Engineering Journal. 2022; 437: 135338. doi: 10.1016/j.cej.2022.135338
109. Zhou T, Pang WK, Zhang C, et al. Enhanced Sodium-Ion Battery Performance by Structural Phase Transition from Two-Dimensional Hexagonal-SnS2 to Orthorhombic-SnS. ACS Nano. 2014; 8(8): 8323–8333. doi: 10.1021/nn503582c
110. Sahoo BB, Pandey VS, Dogonchi AS, et al. Synthesis, characterization and electrochemical aspects of graphene based advanced supercapacitor electrodes. Fuel. 2023; 345: 128174. doi: 10.1016/j.fuel.2023.128174
111. Miao J, Zhu Q, Li K, et al. Self-propagating fabrication of 3D porous MXene-rGO film electrode for high-performance supercapacitors. Journal of Energy Chemistry. 2021; 52: 243–250. doi: 10.1016/j.jechem.2020.04.015
112. Moatasim M, Wang Z, Xie Y, et al. Solving Gravimetric-Volumetric Capacitive Paradox of 2D Materials through Dual-Functional Chemical Bonding-Induced Self-Constructing Graphene-MXene Monoliths. ACS Applied Materials & Interfaces. 2021; 13(5): 6339–6348. doi: 10.1021/acsami.0c21257
113. Fan Z, Wang Y, Xie Z, et al. Modified MXene/Holey Graphene Films for Advanced Supercapacitor Electrodes with Superior Energy Storage. Advanced Science. 2018; 5(10). doi: 10.1002/advs.201800750
114. Shao L, Xu J, Ma J, et al. MXene/RGO composite aerogels with light and high-strength for supercapacitor electrode materials. Composites Communications. 2020; 19: 108–113. doi: 10.1016/j.coco.2020.03.006
115. Yan J, Ren CE, Maleski K, et al. Flexible MXene/Graphene Films for Ultrafast Supercapacitors with Outstanding Volumetric Capacitance. Advanced Functional Materials. 2017; 27(30). doi: 10.1002/adfm.201701264
116. Yang X, Wang Q, Zhu K, et al. 3D Porous Oxidation-Resistant MXene/Graphene Architectures Induced by In Situ Zinc Template toward High-Performance Supercapacitors. Advanced Functional Materials. 2021; 31(20). doi: 10.1002/adfm.202101087.
117. Cao B, Zhang Q, Liu H, et al. Graphitic Carbon Nanocage as a Stable and High Power Anode for Potassium-Ion Batteries. Advanced Energy Materials. 2018; 8(25). doi: 10.1002/aenm.201801149
118. Ganiyat Olatoye A, Li W, Oluwaseyi Fagbohun E, et al. High-performance asymmetric supercapacitor based on nickel-MOF anchored MXene//NPC/rGO. Journal of Electroanalytical Chemistry. 2023; 928: 117036. doi: 10.1016/j.jelechem.2022.117036
119. Gao T, Li H, Zhou F, et al. Mesoporous carbon derived from ZIF-8 for high efficient electrosorption. Desalination. 2019; 451: 133–138. doi: 10.1016/j.desal.2017.06.021
120. Jiang G, Zheng N, Chen X, et al. In-situ decoration of MOF-derived carbon on nitrogen-doped ultrathin MXene nanosheets to multifunctionalize separators for stable Li-S batteries. Chemical Engineering Journal. 2019; 373: 1309–1318. doi: 10.1016/j.cej.2019.05.119